LUNDS UNIVERSITET

Lunds Tekniska Högskola

MASTER THESIS

Engineering HMF oxidoreductase for efficient furan building block production

December 2023- May 2024

NEHA GUPTA

Degree Project in Biotechnology (30ECTS)

Examiner: Dr. Rajni Hatti Kaul

Supervisor: Dr Mohamed Ismail

Acknowledgement

I extend my sincere appreciation to Dr. Mohamed Ismail, my dedicated supervisor, whose unwavering support and encouragement have been pivotal throughout the journey of my thesis. His guidance and mentorship have been invaluable, shaping my research and contributing significantly to my academic development.

I am profoundly thankful for Dr. Rajni Hatti-Kaul's invaluable input and guidance, which have significantly influenced the trajectory of my research. Additionally, I am grateful for the opportunity she provided me to join the STEPS Spring meet-up, where I had the privilege of presenting a poster showcasing a portion of this work.

I would like to express my gratitude to Dr. Mahmoud Sayed Ali Sayed and Dr. Adel Elsayed Attia Abouhmad for their valuable contributions and insightful comments. Their thoughtful input has enriched the discussion and enhanced the quality of my work.

I want to give a big thank you to the Department of Biotechnology at Lund University. They've been incredibly supportive, helping me with all the chemicals and equipments needed to finish my project successfully. Their commitment to ensure my research goes smoothly has been really important in helping me achieve my goals.

Additionally, I wish to express my profound gratitude to my friends and family for their unwavering support and encouragement, which have sustained me through the challenges and triumphs of this academic pursuit.

To each of you who have contributed to my research journey and achievements, I offer my heartfelt thanks. Your collective efforts have played a crucial role in shaping my academic endeavors and successes.

Table of Contents

1 Popular Science Summary:

Plastic is a word which is derived from the Greek word ‘plastikos’ meaning capable of being shaped or molded. Now a days the word ‘plastic’ extends for a category of petrochemical materials called polymers. Polymers, which consist of long chains of molecules, are abundant in nature, with cellulose being a common natural example found in plant cell walls. Over the past 150 years, humans have developed the ability to create synthetic polymers, often derived from petroleum and other fossil fuels rich in carbon atoms. These synthetic polymers feature extended molecular chains, giving them strength, lightness, and flexibility, the qualities that define their plasticity. As a result, synthetic polymers have become essential in various aspects of modern life, profoundly influencing the way we live, especially over the last five decades. Over the years plastics reputation declined as concerns about waste increased. Plastic became a major focus because, despite many products being disposable, plastic persists in the environment indefinitely. The plastics industry proposed recycling as a solution and led a significant campaign in the 1980s to encourage cities to collect and process recyclable materials. However, recycling isn't perfect, and most plastics still end up in landfills or as litter.

Problems around plastic production has emerged due to the growing concerns about rapid depletion of fossil fuel reserves, environmental issues, the desire to reduce greenhouse gas emissions, the shift towards a circular economy model and most importantly their potential health risks. These worries center on additives like bisphenol A (BPA) and phthalates, used to make plastics more flexible, durable, and clear. Some scientists and members of the public are concerned that these chemicals can leach into food, water, and our bodies, potentially disrupting the endocrine system at high doses. Researchers are particularly worried about the impact on children and the long-term effects of these chemicals accumulating in the environment.

Despite rising concerns, plastics are crucial to modern life, enabling the development of electronics, medical advances and transportation. They make many products affordable and accessible. Given their value, scientists are working to make plastics safer and more sustainable. Some are developing bioplastics from plant materials rather than fossil fuels, aiming for more environmentally friendly alternatives. Others focus on creating truly biodegradable plastics.

Traditional plastics contain PET, which stands for Polyethylene Terephthalate. PET is a versatile polymer used in packaging industry. Studies have revealed that PET can be replaced by polyethylene furanoate (PEF), a promising, eco-friendly biobased alternative with a reduced environmental impact. To create PEF, the essential ingredient is HMF (5-Hydroxymethylfurfural), a chemical obtained from plants such as corn or sugar. HMF undergoes a conversion process to become FDCA (furandicarboxylic acid), which is later mixed with ethylene glycol to form PEF. This process makes PEF not only plant-based but also more sustainable, as it can break down more easily than PET, offering a greener solution for our plastic needs. HMF undergoes oxidation to form HMFCA, which then polymerizes with ethylene glycol to create PEF.

This research focused on protein engineering of an enzyme called HMF/furfural oxidoreductase (HMFH), which plays a key role in transforming HMFCA into FDCA, a building block for PET.

It was found that the enzyme HMFH works better in one type of broth called TB rather than another called LB. Additionally, adding a tag called MBP to the enzyme makes it work even better. The study focused on evaluating the performance of the enzyme by introducing specific genetic changes. Thorough research, combined with bioinformatics tools, identified 12 genetic alterations for the enzyme. After simulation analysis, 6 mutations were selected for further investigation. One of the mutations showed that the enzyme could convert the substrate completely, although less efficiently than the wild type. Conversely, another mutation greatly diminished the enzyme's effectiveness, emphasizing the crucial role of these specific residues in enzyme activity and how altering them disrupts the enzyme's function. Having seen the impact of genetic alterations on enzyme efficiency, further research with the remaining 4 alterations can refine enzymatic activity. By selecting the most effective mutation, we can then upscale production of FDCA, facilitating large-scale manufacturing of PEF or bioplastics.

2 Abstract:

As the demand for eco-friendly alternatives to traditional plastics grows, Polyethylene Furanoate (PEF) emerges as a promising solution. Derived from renewable biomass sources, PEF embodies sustainability principles by reducing reliance on finite resources and minimizing environmental impact. PEF is synthesized from 2,5-furandicarboxylic acid (FDCA), a key monomer which upon polymerization has the potential to form a variety of bioplastics. The main challenge faced is the low yield of FDCA. To cope with the increasing demand for biobased alternatives, the FDCA production pathway needs to be engineered. The synthesis of FDCA from 5-Hydroxymethyl-2-furancarboxylic acid (HMFCA), mediated by the HMF oxidoreductase (HMFH) gene presents a significant bottleneck. HMFCA successful transformation is critical for the overall process. This study aims to enhance the efficiency of HMFH by employing protein engineering techniques including docking, molecular dynamics simulations, and site-directed mutagenesis. Through mutagenesis, significant findings emerged regarding the Thr550Ser and Met58Pro mutants. The wild type showed higher activity than the mutants. Thr550Ser mutant showed nearly complete oxidation of HMFCA, indicating catalytic activity or substrate binding, but to a lesser extent. On the other hand, the Met58Pro mutant exhibited negligible HMFCA oxidation, suggesting a substantial disruption in catalytic behaviour. These observations underscore the impact of mutations on enzyme activity and substrate specificity, offering insights for enzyme optimization in biotechnological applications. To further improve the enzyme's catalytic efficiency and substrate affinity, additional mutation testing could target the D46G, S204G-Y209V, Y209V and V21C mutations. This research contributes to the advancement of sustainable methods for furan building block production, addressing the pressing need for environmentally friendly alternative to fossil-based plastics.

Keywords:

Bioplastics; catalytic activity; enzyme optimization; environmentally friendly alternatives; FDCA; furan building block production; HMF oxidoreductase (HMFH) gene; polyethylene furanoate (PEF); protein engineering; substrate specificity; sustainable methods.

3 Abbreviations:

E. coli	*Escherichia coli*
FAD	Flavin Adenine Dinucleotide
FFCA	5-formyl-2-furancarboxylic acid
FDCA	2,5-Furandicarboxylic acid
g	Grams
g/L	Grams per litre
h	Hour
HMF	Hydroxymethylfurfural
HMFCA	5-hydroxymethyl-2-furancarboxylic acid
HMFH	HMF/furfural oxidoreductase
HMFO	5-(hydroxymethyl)furfural oxidase
IPTG	Isopropyl β- d-1-thiogalactopyranoside
Kb	Kilo base
L	Litre
L/min	Litres per minute
LB	Lauria-Bertani medium
M	Moles per litre
MBP	Maltose-Binding Protein
min	Minutes
OD	Optical density
PCR	Polymerase chain reaction
rpm	Revolutions per minute
SUMO	Small ubiquitin-related modifier
TB	Terrific Broth medium
UV	Ultraviolet
V	Volts

4 Background:

Plastic is the most favored product; it has left no stone unturned in making its usage indispensable in the world. It possesses unique blend of properties which makes it superior to other packaging materials in the market like durability, versatility, lightweight, chemical resistance, water resistance, insulation, transparency, color ability, recyclability, low cost and many more (1-3) This increasing demand for plastic has led to the increase in production of plastic which is ending up in the landfills, water bodies and other natural resources, due to its non-biodegradable nature. The rate of accumulation of this non-biodegradable plastic has become an alarming problem leading to widespread pollution, ecosystem degradation and threats to aquatic life, wildlife, and human health (4-10). Hence there is a need to find a suitable alternative which will possess the functionalities of plastic and at the same time will not pose a threat to the environment. Finding an alternative with this unique combination is challenging.

To address this situation, researchers have come up with the sustainable alternative called bioplastics (11-15). These are a kind of plastic derived from renewable biomass sources such as plants, by-products of agriculture, microorganisms etc. The bioplastics are considered a safe alternative because of their lower reliance on limited resources and less environmental interference (16-22). There are various types of bioplastics depending on their application like Polylactic Acid (PLA), Polyhydroxyalkanoate (23), Polyethylene furanoate (PEF), Polyhydroxybutyrate (PHB). The Polylactic Acid (PLA), derived from renewable resources like sugarcane and corn starch, finds extensive use in various applications such as packaging, tableware and implants due to its biodegradable nature. Polyhydroxyalkanoate, produced through bacterial fermentation of organic substrates, serves in printing, packaging and medical devices offering biocompatibility and environmental friendliness. Polyethylene Furanoate (PEF), from plant-based sugars, is employed in production of beverage bottles and food packaging owing to its biodegradability and enhanced barrier properties. Polyhydroxybutyrate (PHB), synthesized via bacterial fermentation of sugar or lipids, is favored for packaging materials and disposable items, contributing to the reduction of plastic waste through its biodegradable property (16, 17, 19-22, 24, 25).

PEF is derived from the biochemical pathway which involves the conversion of biomass into FDCA which serves as the key building block of bioplastic production. In this pathway the biomass or glucose is isomerized to form fructose which upon dehydration results in formation of HMF, which serves as the key intermediate (2, 26-30). This HMF undergoes selective oxidation of hydroxyl moiety and aldehydic moiety by different enzymes. The oxidation of hydroxyl moiety leads to formation of 2,5-diformylfuran (DFF) while the oxidation of aldehydic moiety results in HMFCA. Both DFF and HMFCA are oxidized to form FFCA which is further oxidized to form 2,5- furandicarboxylic acid (FDCA) (Fig 1) (25, 27, 31) The FDCA undergoes esterification with diols such as ethylene glycol forming furanoate esters. These esters then polymerize to produce PEF (polyethylene furanoate), a bioplastic material with wide industrial potential (2, 3, 6, 16, 17, 32, 33). The studies are still going on to find a suitable approach to enhance the production of bioplastics. One such bottleneck identified is the production of FDCA via HMFCA using HMFH as the oxidoreductase enzyme (2, 23, 25, 28-30, 34-36). In this pathway, the HMFCA is not efficiently converted to FDCA hence it aims to engineer HMFH enzyme using protein engineering techniques by site directed mutagenesis and evaluate the conversion using HPLC technique (37).

HMF oxidase (HMFO) from Methylovorus sp. strain MP688 effectively converts HMF to FDCA(15, 25, 28, 29, 31, 36). HMFO demonstrates efficient catalysis, broad substrate activity, and thermostability, making it suitable for eco-friendly FDCA production. Previous studies have indicated improved thermostability of HMFO through computational approaches and novel gene shuffling methods, resulting in a highly efficient and stable variant capable of industrially relevant FDCA production from 5-hydroxymethylfurfural (HMF)(29, 31, 38). HMFO is similar to fungal aryl-alcohol oxidases (AAOs) but has distinct substrate specificity. It efficiently oxidizes HMF and various benzylic compounds, favoring those with primary alcohol groups. Its active site architecture allows for selective alcohol and aldehyde oxidations. While structurally different from fungal AAOs, HMFO shares catalytically important residues. Recently, HMF oxidase activity was discovered in *Cupriavidus basilensis*. This enzyme, HmfH, belongs to the GMC oxidoreductase family and is involved in metabolizing HMF. Although its exact substrates and products are still unknown, when introduced into *Pseudomonas putida*, it enables FDCA production from HMF, suggesting its potential for alcohol and aldehyde oxidations. HmfH likely utilizes flavin adenine dinucleotide (FAD) as a cofactor, typical for GMC oxidases, and its activity extends beyond HMF to other aromatic substrates. These unique abilities make it a promising biocatalyst for green chemistry applications, including the production of FDCA from HMF(39, 40).

Around 6 mutations have been designed by molecular docking using YASARA tool (39, 40). The HMFH enzyme doesn't have experimentally determined 3D structure in Protein Data Bank (PDB). Hence predicted structure was used for mutation analysis of HMFH. It has around 51.57% sequence identity with HMFO which is a flavoprotein with FAD as co enzyme (25, 28, 29, 31, 35, 36, 41, 42). The research focuses on advancing the production of a crucial furan building block through a multi-step process involving various oxidation stages, targeting a critical bottleneck. 5-hydroxymethylfurfural (HMF), derived from sugars, holds potential as a renewable chemical building block, especially for the synthesis of 2,5-furandicarboxylic acid (FDCA) via selective oxidation. We intend to achieve this by employing protein engineering techniques, specifically focusing on HMF oxidoreductase (HMFH), the enzyme responsible for catalyzing the problematic step, with the goal of enhancing the efficiency of the conversion process using a sustainable approach.

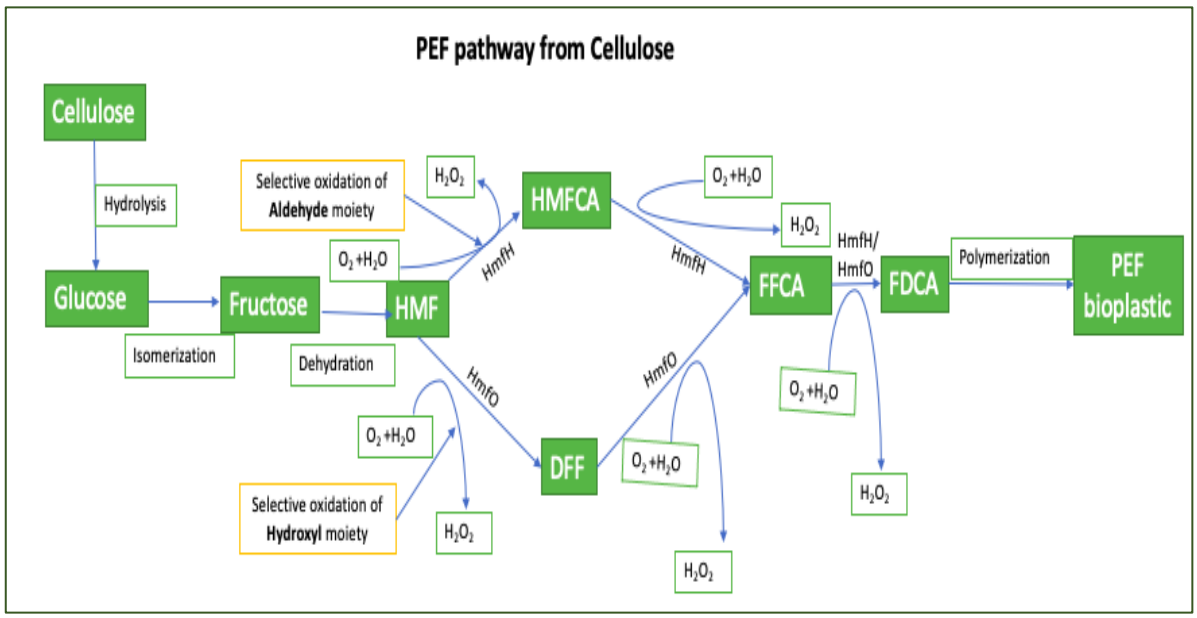

Fig 1: PEF bioplastic pathway derived from Cellulose.

5 Aims:

- Determine best HMFCA concentration (0.5-5 mg/ml) for oxidation by HMFH
- Identify optimal medium for HMFH (LB or TB)
- Compare activity of wild type with HMFH variants tagged with SUMO and MBP
- Evaluate different cell lysis methods
- Identify mutations that significantly affect the enzymatic activity of HMFH.
- Amplify and confirm mutants
- Compare activity of wild type and mutants with/without FAD

6 Materials and methods:

6.1 Medium preparation:

For LB medium, Tryptone 10g, NaCl 10g, Yeast extract 5g was added to H_2O such that final volume accounted to 1L. The pH was adjusted to 8.0 with 2M NaOH and 6M HCl. For TB medium, 900 mL of TB medium containing (12g/L Tryptone, 24 g/L yeast extract, 5 g/L glycerol) was added to 100 mL of 10X TB salt containing 23.1 g/L of 0.17 M KH_2PO_4, 125.4 g/L of 0.72 M K_2HPO_4.

6.2 Cultivation of HMFH wildtype and variants:

Preculture preparation:

Precultures in LB and TB medium were prepared using the glycerol stock of HMFH/ HMFH SUMO/ HMFH MBP in *E. coli* BL21 (plasmid) were provided by the department of Biotechnology at Lund University for this study. For LB preculture, 20 µL of HMFH gene was inoculated into 25 mL of LB medium supplemented with 25 µL of Kanamycin (50 µg/mL) or Ampicillin (100 µg/mL) for TB preculture. The cultures were incubated at 37°C for 15 hours, and the optical density (OD) at 600 nm was measured. Dilution factor 50 (DF50) was applied to calculate the final OD.

Glycerol stock:

Glycerol stocks were prepared by adding 500 µL of HMFH preculture to 500 µL of 40% glycerol and storing at -20°C.

Inoculum preparation:

The amount of preculture required for the final inoculum was calculated based on the desired 0.1 OD. Cultures were incubated until reaching an OD_{600nm} of 0.6, indicating logarithmic growth phase. Protein expression was induced with 0.15 mM IPTG and kept in a shaker at 16°C for 48 hours.

Cell harvesting:

500 µL of culture was collected for OD measurement. The culture was centrifuged using Sigma 3-16PK, Sigma, Germany, at 12000 rpm at 4°C for 30 mins. Discard all the supernatant leaving behind the pellet at the bottom.

Cell lysis:

Performed alternate methods of lysing the cells by chemical means using Bugbuster, sound energy using a sonicator.

Bug Buster:

To achieve a final concentration of 10 mg/mL cells dry weight, 2 mL of HMFH MBP (initial concentration: 23.023 mg/mL cell dry weight in phosphate buffer) was suspended in 3 mL of phosphate buffer. The concentration of HMFH Sumo was adjusted to match that of HMFH MBP (23.023 mg/mL cell dry weight), and then 2 mL of HMFH Sumo was suspended in 3 mL of Phosphate buffer to obtain a concentration of 10 mg/mL cells dry weight. The cell lysis procedure adhered to the protocol outlined in the BugBuster® Protein Extraction Reagent guidelines provided by Novagen.

Sonication:

To perform sonication Fisherbrand™ Q505 Sonicator from ThermoFisher Scientific was used. To achieve a final concentration of 10 mg/mL cells dry weight, 2 mL of HMFH MBP (initial concentration: 23.023 mg/mL cells dry weight in phosphate buffer) and 2 mL of HMFH Sumo (initial concentration: 23.023 mg/mL cells dry weight) were each suspended in 3 mL of phosphate buffer. In total, 5 mL of cells containing HMFH Sumo and HMFH MBP at a concentration of 10 mg/mL cells dry weight were prepared for sonication. The cell pellet was initially resuspended in phosphate buffer at pH 8.0 to a total volume of 5 mL. Throughout the process, the falcon tubes were carefully kept on ice to maintain the temperature. Subsequently, sonication was performed for 10 minutes at 60 amplitude and 0.5 cycle. Following sonication, the viscosity of the solution was assessed, and if necessary, sonication was extended for an additional 10 minutes until the solution reached a less viscous state. Upon completion of sonication, the solution was evenly distributed into Eppendorf tubes, with each tube containing 2 mL . Centrifugation was then carried out using Sigma 3-16PK, Sigma, Germany, at 15000 rpm for 30 minutes at 4°C. After centrifugation, the soluble fraction was meticulously collected in new Eppendorf tubes and subsequently filtered using a 0.22 filter to remove any remaining solid particles. Finally, the insoluble fraction was resuspended in phosphate buffer, using the same volume as that collected in the soluble fraction.

6.3 Activity assay for HMFCA oxidation:

The reaction mixture comprised 3mL of enzyme (10mg/mL cells dry weight), 150µL of HMFCA 40mg/mL (resulting in a concentration of 2mg/mL in 3mL), and 150µL of FAD 0.828mg/mL (equating to 50uM or 0.0414mg/mL in 3 mL). Samples for HPLC analysis were prepared by combining 100µL of reaction sample, collected at various time points (T0, T3, T24, T48, T51), with 1900 µL of Milli-Q H2O and 40µL of 10% H2SO4. The peaks corresponding to the different compounds were confirmed and quantified using external standards for comparison. The concentrations of HMFCA, FFCA, and FDCA were analyzed using HPLC (JASCO, Tokyo, Japan), equipped with a fast acid analysis chromatographic

column connected to a guard column (Biorad, Richmond, CA, USA). Detection was facilitated by a refractive index detector (ERC, Kawaguchi, Japan) and a JASCO UV detector operating at 254 nm. Additionally, a JASCO intelligent autosampler was utilized. During the analysis, the column temperature was maintained at 65°C in a chromatographic oven (Shimadzu, Tokyo, Japan).

6.4 In vitro mutagenesis of HMFH:

Inoculum:

A preculture of HMFH MBP was prepared in a 50mL falcon tube using 10mL of LB medium, 10 µL of Ampicillin (100 mg/mL) and 10 µL glycerol stock of HMFH MBP in LB medium was provided by the Department of Biotechnology at Lund University for this study. It was kept at 37 °C for 16 hrs in shaking incubator (Electron, Infors HT, UK) at 200 rpm.

Plasmid Extraction:

A preculture of HMFH MBP was prepared in a 50mL falcon tube using 10mL of LB medium,10 µL of Ampicillin (100mg/mL) and 10 µL glycerol stock of HMFH MBP in LB medium. It was kept at 37 °C for 16 hrs in shaking incubator (Electron, Infors HT, UK) at 200 rpm.

Primers:

The primers listed in Table 1 were received from Integrated DNA technologies and first centrifuged for 20 secs as the primers may have been dislodged during shipping. Milli-Q water was added in an equivalent amount to adjust the final concentration to 100 µM. 10 µl of each primer was then taken in 1.5 mL Eppendorf tube and then 90 mL of milliQ water was added to make the concentration from initial 100 µM to 10 µM. It was kept at -20 °C in freezer.

Table 1 Mutation sequences

Mutation Code	Mutation	Forward sequence	Reverse sequence
M1	HMFH D46G	5'- ACC CCA CCT **GGC** GCT GTT CCC -3'	5'- ATC AAC ACC GGC TTC GAT CAA GGC- 3'
M2	HMFH-S204G-Y209V	5'-AT AAA CGA GTA **GGC** ACA GCC ATT GCT **GTT** CTG GAT G -3'	5'- CAT CCA AGT TCG AGA AAG CAG CAG G -3'
M3	HMFH V21C	5'- G TCT GCG GGG TGT **TGC** TTG GCT AAT CGT -3'	5'- CCA CCG CCC ACA ATT ACA TAA TCA AAC CGT -3'
M4	HMFH-D200T-Y209V	5'- CA GCC ATT GCT **GTT** CTG GAT GCG G -3'	5'- T TGA TAC TCG TTT **GGT** ATC CAA GTT CGA GAA AGC AG -3'

M5	HMFH T550S	5'-CT AAT ACT AAT ATC **AGC** ACT ATC ATG CTT GCG GAG AAA A-3	5'- CTG TAG GCA AAC GCG GCA TCA AGC -3'
M6	HMFH M58P	5'- GAC AGT TAT CCG **CCG** CCC TTG TTC TTC -3'	5'- GAG GAT CTC AGC GGG AAC AGC GTC -3'

5' Phosphorylation of Primers:

Ten µL of 100 mM ATP was added in 90 µL of nuclease free water resulting in 10 mM ATP. Five µL of reaction buffer A for T4 polynucleotide kinase purchased from Thermo Scientific™, 5 µL of 10 mM ATP, 2 µL of T4 Polynucleotide kinase 10 U/ µL, 250 pmol of forward / reverse primer. The reaction was incubated at 37 °C for 30 minutes. The phosphorylated primers were stored at -20 °C.

Gradient PCR:

For gradient PCR the reaction was prepared using 27.5 µL milli Q H_2O, 10 µL 5X Phusion Buffer, 1 µL of 10 mM DNTPs, 1 µL of Plasmid, 5 µL phosphorylated Forward Primer, 5 µL reverse phosphorylated primer, 0.5 µL of Phusion Hot start polymer. It was carried out at different temperature gradients like 73.2 for M1, 71.7 for M2, 74.7 for M3, 72 for M4, 72 for M5 and 72 for M6 (Table 2).

Table 2 Mutation melting temperature:

Mutation	Melting Temperature °C (Tm)
HMFH D46G	73.2
HMFH 204-209	71.7
HMFH V21C	74.7
HMFH Y200-9V	72
HMFH T550S	72
HMFH M58P	72

PCR:

A master mix was prepared using 10µL of DNTPs, 350 µL of milliQ water, 100 µL of buffer, 10 µL of 10 mM plasmid (template) accounting to 480 µL. For each reaction 48 µL of this master mix was used. To the 7 PCR reaction tubes, 48 µL of master mix, along with 1.25 µL of forward and 1.25 µL of reverse primer, 1 µL of 10 mM plasmid were added to each tube.

Competent cell preparation using rubidium chloride:

The competent cells were prepared by growing an overnight culture from a glycerol stock in LB medium at 37°C with shaking. Following this, the entire overnight culture was transferred to a baffled flask and allowed to grow until the A600 reached 0.4–0.6. The cells were then pelleted by centrifugation and gently resuspended in ice-cold TFB1. After a 20-minute incubation on ice, the cells underwent another round of pelleting and were subsequently resuspended in ice-cold TFB2. Following an additional incubation period of 15–60 minutes on ice, the resuspended cells were aliquoted into prechilled tubes and stored at -80°C. Throughout the process, the cells were handled gently due to their sensitivity to both handling

and elevated temperatures. Patience and gentle handling were required for resuspending cells in TFB1, whereas cells resuspended more easily in TFB2. This method typically yielded excellent competency (1.5x107) and allowed cells to be stored for up to a year. Finally, a heat shock was performed for 60 seconds at 42°C.

7 Results:

7.1 Determine the best HMFCA concentration (0.5-5 mg/mL):

The evaluation of HMFCA oxidation after 48 hours using HMFH MBP whole cells (30 mg/mL cells dry weight) in the presence of FAD (50 µM) with various HMFCA concentrations (0.5, 1, 2, 3, 4, 5 mg/mL) was examined, focusing on the formation of FFCA and FDCA. Among the different HMFCA concentrations tested, 2 mg/mL was identified as the most suitable concentration, as it was totally oxidized after 24 hours and completely converted to FFCA and FDCA after 48 hours (Fig 2)

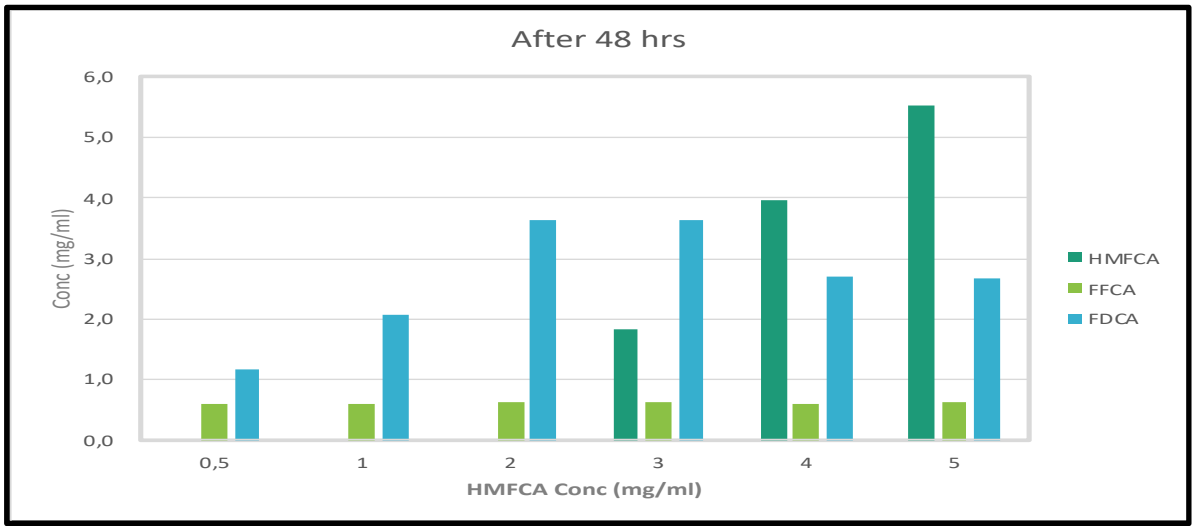

Fig 2: Effect of different substrate concentrations on HMFCA oxidation

7.2 Identify the optimal medium for HMFH (LB or TB):

The concentration of HMFH MBP was 12 mg/mL cells dry weight in TB medium and 10 mg/mL cells dry weight in LB medium. Interestingly, a noticeable decrease in HMFCA conversion was observed in TB medium compared to LB medium. This suggests that HMFCA conversion is more favorable in LB medium (Fig 3).This suggests that the conversion of HMFCA is more favorable in TB medium.

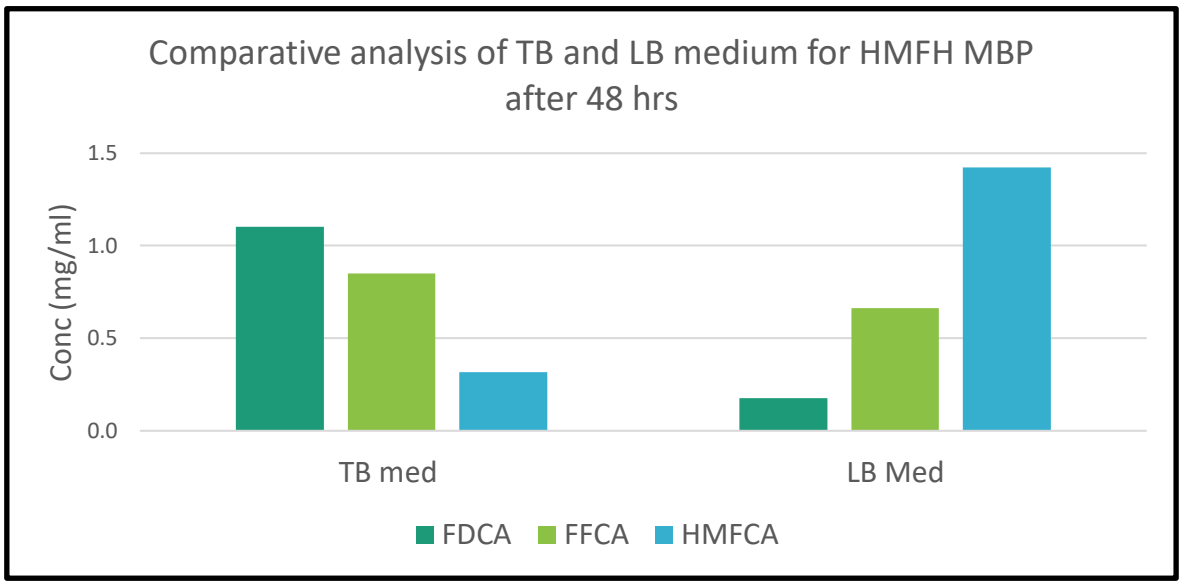

Fig 3: Comparative analysis HMFH MBP whole cells in TB and LB medium after 48 hrs

7.3 Compare the activity of tagged HMFH variants:

Upon comparing the enzymatic activity of wild-type HMFH and variants tagged with SUMO and MBP whole cells it was found that even at low concentration HMFH MBP showed efficient conversion compared to SUMO and Wild type (Fig 4).

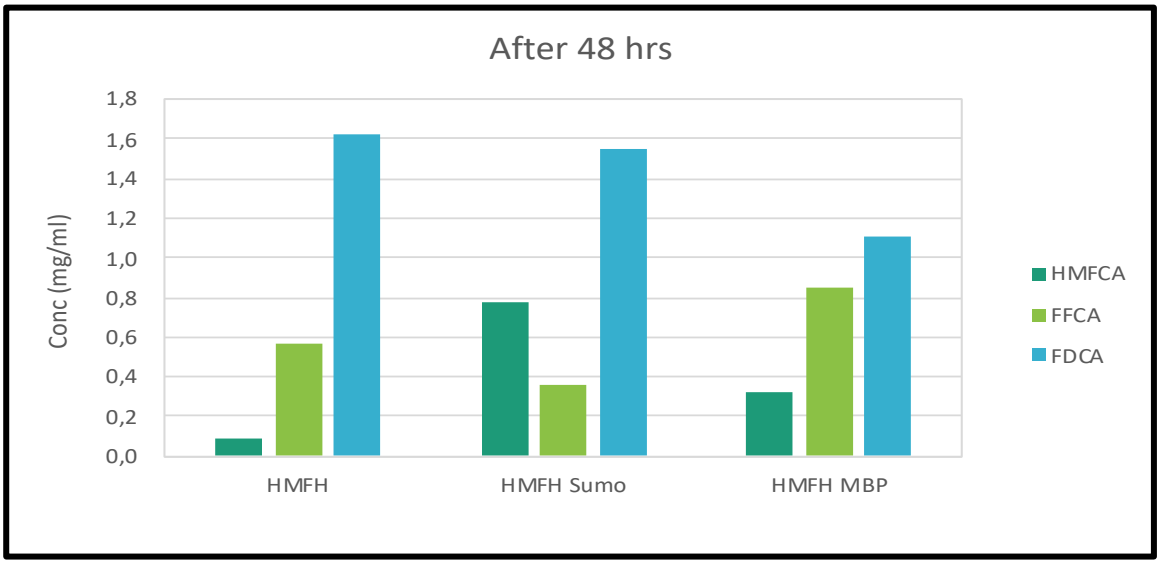

Fig 4: Comparative analysis of the enzymatic activity of wild-type HMFH and variants tagged with SUMO and MBP

7.4 Evaluate different cell lysis methods:

Upon comparing the HMFH wild type whole cells with chemically lysed cells using Bug Buster represented as 'BB' and Sonicated cells represented as 'SC' in the plot it was found that the whole cells showed high conversion rates (Fig 5), (Appendix Fig: A1)

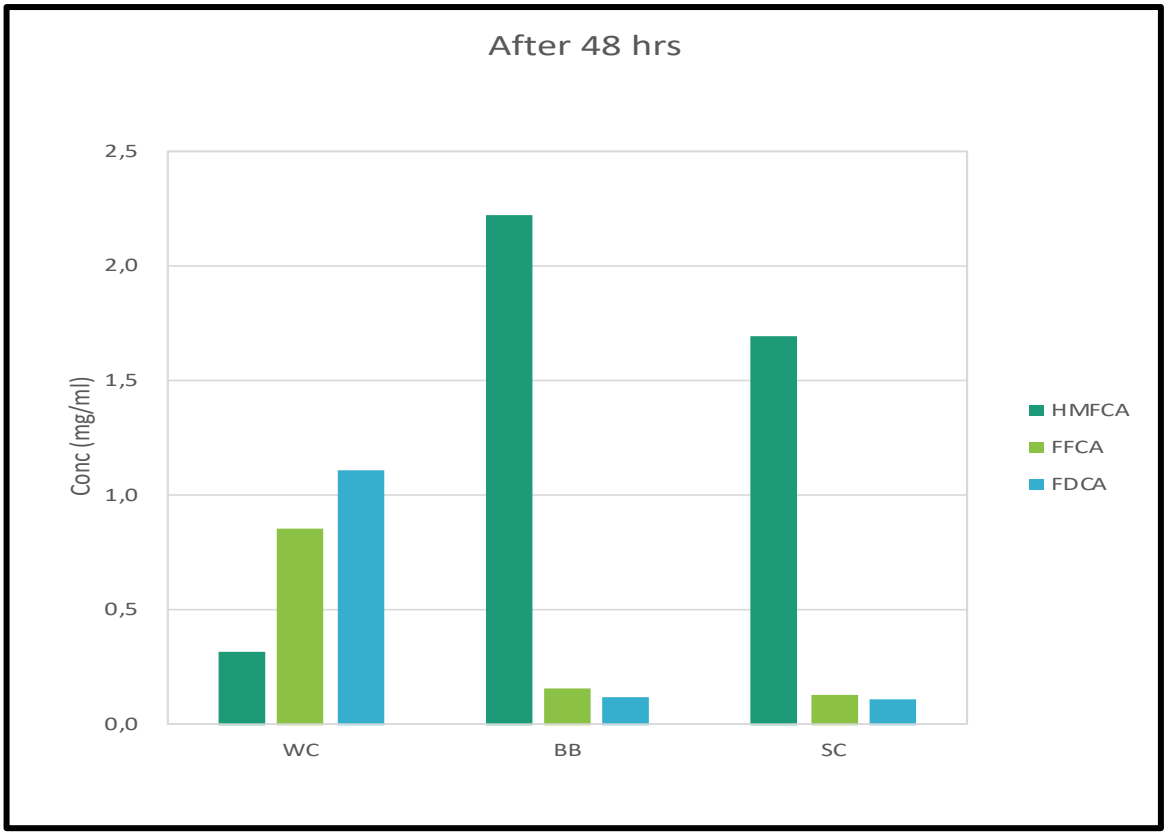

Fig 5: Comparison of HMFCA conversion rates using various lysis methods after 48 hours of incubation in TB medium at 30°C and 200 RPM.

7.5 Comparative Analysis of HMFO & HMFH: Structural Insights into Furan Compound Metabolism:

HMFO (5-Hydroxymethylfurfural Oxidase) was compared with HMFH (Hydroxymethylfurfural Hydrolase) to elucidate the structural and functional differences between these enzymes involved in furan compound metabolism. HMFO catalyzes the oxidation of 5-hydroxymethylfurfural (HMF) to 2,5-diformylfuran (DFF) then to 5-formyl-2-furancarboxylic acid (FFCA) leading to 2,5-furandicarboxylic acid (FDCA), In contrast, HMFH also participates in the oxidation of HMF into its intermediate products like 5-hydroxymethyl-2-furancarboxylic acid (HMFCA), FFCA ultimately leading to the formation of FDCA. Despite catalyzing distinct reactions, both enzymes play vital roles in the conversion of biomass-derived sugars into valuable bio-based chemicals. Comparing HMFO with HMFH structurally allows for an understanding of how these enzymes have evolved to perform their specific functions. Structural comparisons can reveal differences and similarities in their active site architectures, cofactor-binding sites, and overall protein folds, shedding light on the molecular mechanisms underlying their catalytic activities and substrate specificities. Such comparisons provide valuable insights into the enzymatic pathways involved in furan metabolism and bioplastic production, informing enzyme engineering efforts aimed at optimizing their performance for industrial applications. Thus, by comparing HMFO with HMFH, we gain a deeper understanding of the structural basis of their functional diversity and pave the way for biotechnological advancements in bio-based chemical production.

7.6 Identification of mutations to improve the activity of HMFH:

To elucidate the structural and functional differences between HMFO (5-Hydroxymethylfurfural oxidase) and HMFH (Hydroxymethylfurfural oxidoreductase), a comparative analysis was conducted. As a crystal structure for HMFH was not available, AlphaFold generated model was utilized for HMFH based on its amino acid sequence. The structural alignment between HMFO and HMFH has a Calpha RMSD of 0.977 Å over 477 aligned residues with 51.57% sequence identity, indicating a relatively close structural similarity between the two proteins despite their sequence differences (Fig 6). To identify potential cofactor and catalytic binding sites within HMFH, the AlphaFold-generated structure was compared with the known PDB structure of HMFO (PDB entry: 4UDP) using Yasara software. This comparison aimed to understand the structural similarities and differences between HMFO and HMFH, shedding light on the molecular mechanisms underlying their catalytic activities and substrate specificities. Furthermore, by comparing the structural features of HMFO with those of the AlphaFold-modeled HMFH, the key structural motifs and residues involved in catalysis and substrate binding in both enzymes, provided insights into their respective roles in furan compound metabolism.

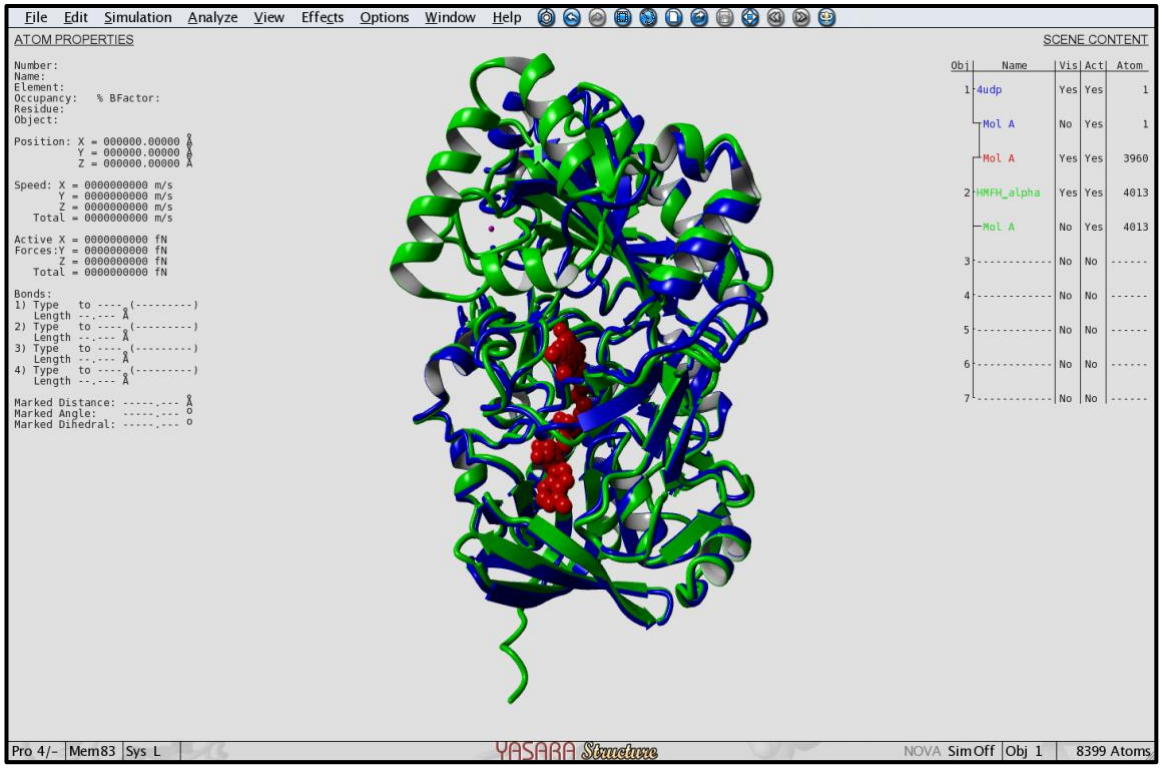

Fig 6: Superimposition of HMFO (FAD bound) with HMFH alpha fold structure using MUSTANG alignment. HMFO (Blue), HMFH (Green) and FAD (Red)

After the superimposition, the HMFO structure was removed, leaving only the FAD bound to the HMFH structure. Subsequently, energy minimization was performed on the HMFH structure to optimize its conformation and reduce any steric clashes or unfavorable interactions. This optimization process resulted in a final energy of -29471.196 kJ/mol after 787 steps of minimization. The HMFCA binding pocket of HMFH was then analyzed to identify active site residues crucial for substrate binding and catalysis. Notably, residues such

as H501, Asn 545, and Val 98 were identified based on their counterparts in the active site of HMFO. These residues play essential roles in positioning the substrate and facilitating catalytic reactions within the enzyme's active site.

The HMFH enzyme is composed of 579 amino acids, encoding the protein's entire sequence and contributing to its structural and functional characteristics. The visualization of the circular map for HMFH MBP, generated with SnapGene Viewer, is displayed in Appendix Figure A2. HMFH, a member of the glucose-methanol-choline (GMC) oxidoreductase protein family, features two distinct conserved domains. The N-terminal GMC domain (Pfam 00732) is crucial for binding the cofactor flavin adenine dinucleotide (FAD), which serves as a prosthetic group. This cofactor enables the oxidative power needed for reactions, with FAD being reduced to FADH− upon substrate oxidation. The reoxidation of the reduced cofactor typically occurs through molecular oxygen, generating hydrogen peroxide alongside the product. In specific GMC flavoprotein oxidases, FAD is covalently linked to a histidine side chain within this domain.

Examination of the binding sites in HMFH revealed three significant areas where flavin adenine dinucleotide (FAD) attaches. These sites are situated at positions 89, 228, and 500-501 within the protein sequence, characterized by the amino acids V, V, and WH, respectively. The second conserved domain, the C-terminal GMC domain (Pfam 05199), is approximately 150 amino acids in length. This domain contains the active-site residues such as Asn 545 and Val 98 including a strictly conserved histidine His 501, which plays a vital role in catalysis.(Fig: 7,8,9).

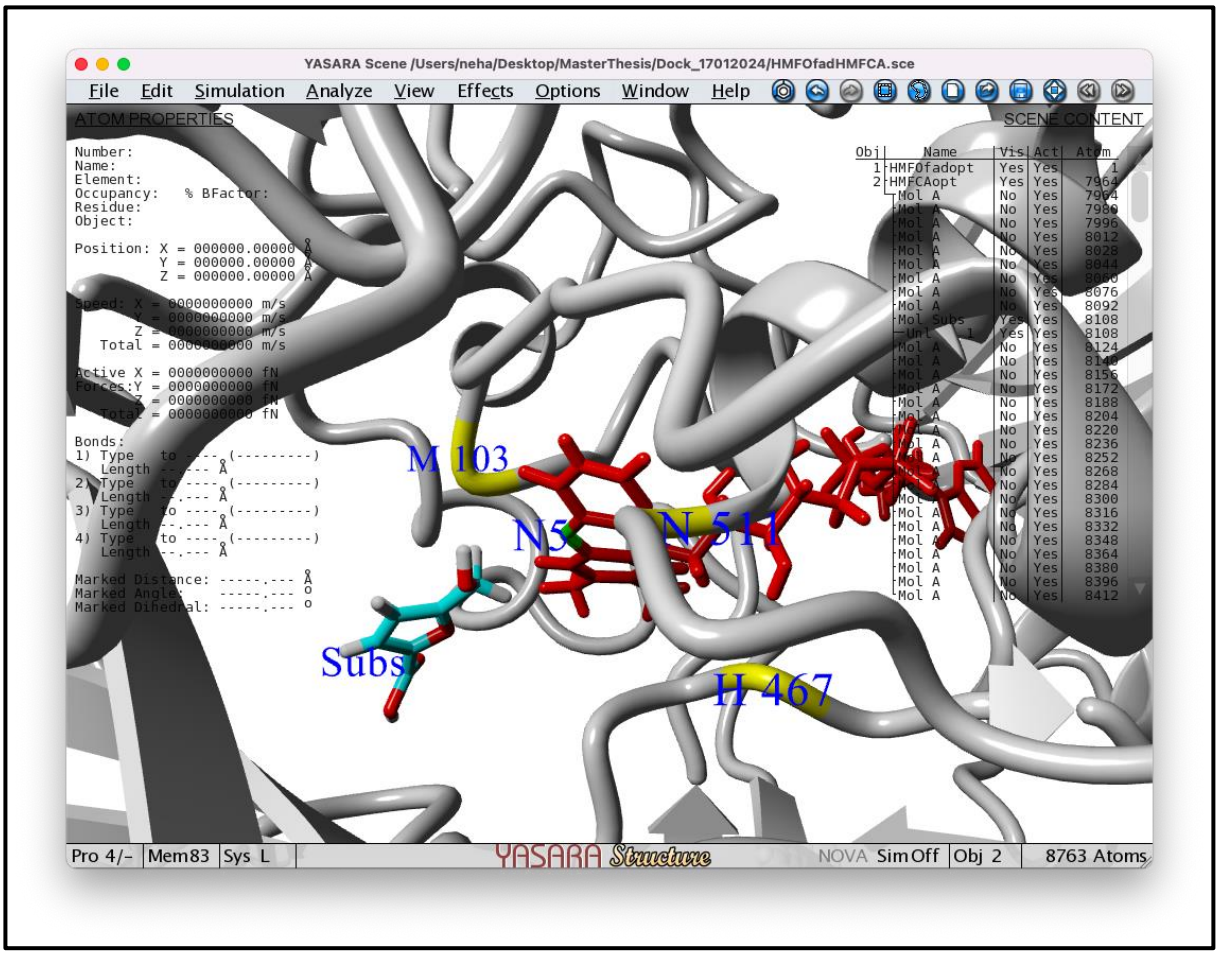

Fig 7: HMFCA substrate docking pose (light blue colour) in the active site of the HMFO using YASARA.

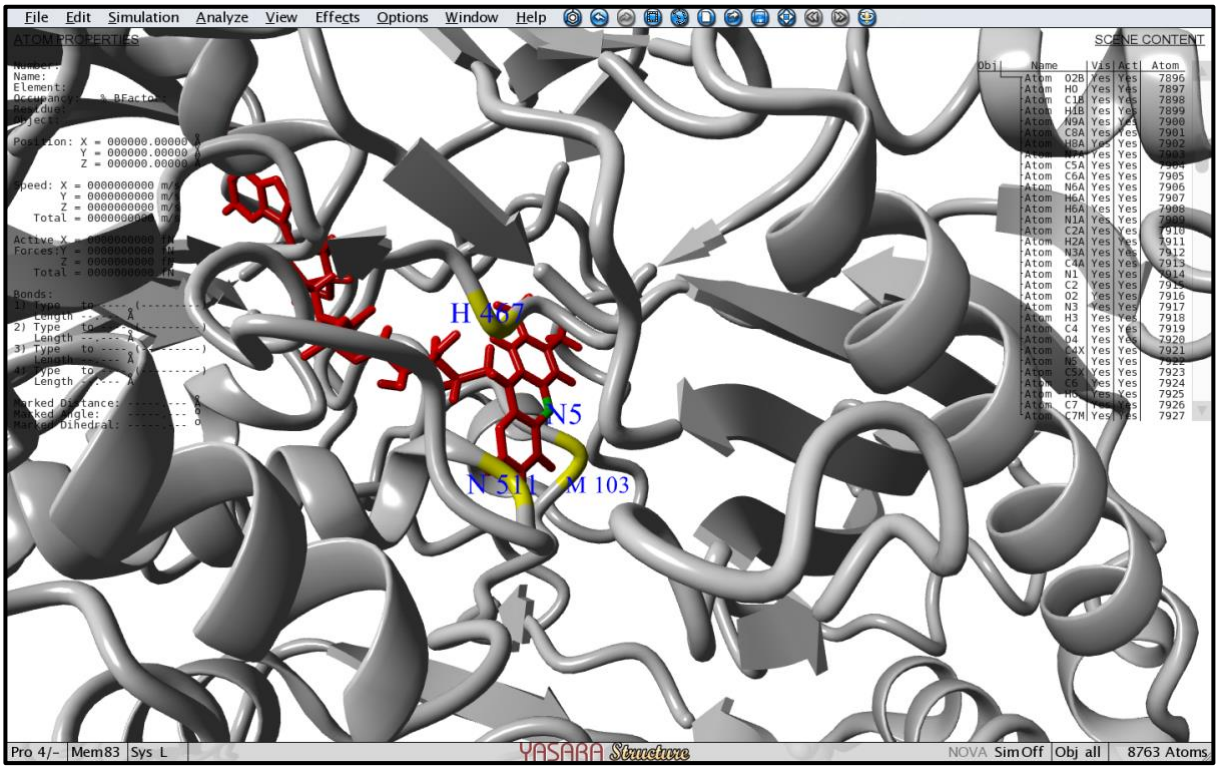

Fig 8: HMFO active site showing N5 position of the FAD in green and all the residues H467, N511 and M103 in yellow.

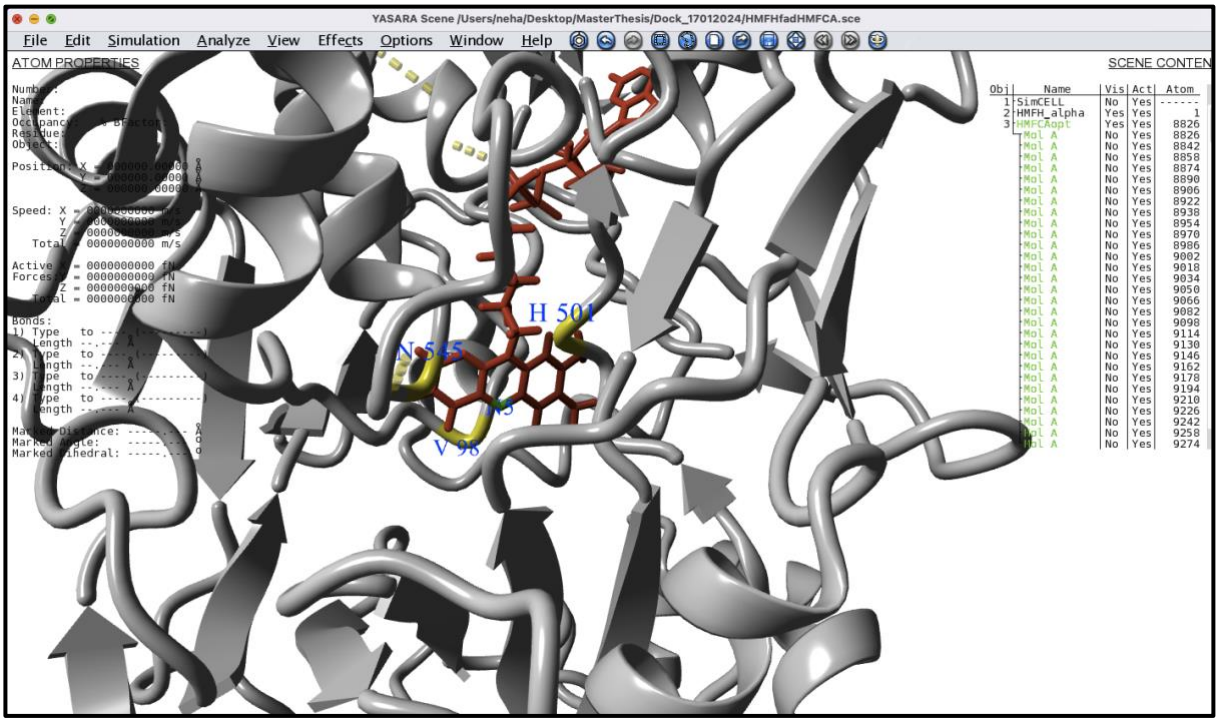

Fig 9: The substrate HMFCA binding pocket of HMFH displaying the active site residue H501, and other residues for the proper positioning of the substrate N545 and V98. The residues were selected as per the corresponding residues in the active site of HMFO. His 467 in HMFO corresponds to His 501 in HMFH, Asn 511 corresponds to Asn 545 and Met 103 corresponds to Val 98.

Energy minimization was conducted using the AMBER99 force field, followed by molecular dynamics simulations using the built-in macro md_run.mcr provided by Yasara Structure software.The simulations were run for at least 1000 ps after necessary preparation steps, including the addition of water molecules, cell neutralization, and pKa prediction at pH 7.4. Finally, all structures underwent energy minimization before further analysis, ensuring their stability and reliability for subsequent studies.

Around 5 mutations out of 12 mutations in HMFH MBP were chosen for molecular dynamics (MD) analysis. These mutations, namely Met58Pro, Val21Cys, Thr550Ser, Ser204Gly+Tyr209Val, and Asp200Thr+Tyr209Val, were selected based on an analysis conducted using HotSpot Wizard 3 (Table 3). This web server automates the design of mutations and smart libraries for protein function and stability engineering, as well as annotating protein structures. It integrates structural, functional, and evolutionary data from various bioinformatics databases and computational tools to identify mutagenesis hot spots.

Table 3 Protein engineering mutations selected using HotSpot Wizard 3

Protein engineering Strategies	Mutation
Functional hot spots	Met58Pro
Stability hotspots by structural flexibility	Val21Cys, Thr550Ser
Correlated hotspots	Ser204Gly+Tyr209Val, Asp200Thr+Tyr209Val

These mutations were chosen according to four protein engineering strategies facilitated by the HotSpot Wizard 3:

i. Functional Hot Spots: These are highly mutable residues located within the catalytic pocket and/or access tunnels, represented by the mutation Met58Pro.
ii. Stability Hot Spots by Structural Flexibility: Residues characterized by structural flexibility, represented by the mutations Val21Cys and Thr550Ser.
iii. Correlated Hot Spots: These are pairs of coevolving residues that jointly influence enzyme activity and selectivity. In this case, the mutations Ser204Gly+Tyr209Val and Asp200Thr+Tyr209Val were identified as correlated hot spots.

By utilizing these strategies, the mutations were chosen to target specific regions of the protein to enhance its function and stability, as per the analysis performed using HotSpot Wizard 3.

7.7 Structural changes in protein mutations:

Table 4 summarizes the structural changes observed in the selected protein mutations before and after molecular dynamics (MD) simulations. The "Calpha RMSD" represents the root mean square deviation of alpha carbons between the initial and final structures after MD simulation. "His N to HMFCA OH Proton" indicates the distance between the nitrogen atom of histidine and the proton of the hydroxyl group of HMFCA. "N5 FAD to HMFCA Alpha Carbon" shows the distance between the N5 atom of FAD and the alpha carbon of HMFCA.

Table 4 molecular dynamics simulation of selected mutations

Mutation	Calpha RMSD (structural alignment between before and after MD simulation) (Å)	Distance from His N position to Proton from OH group of HMFCA(Å)	Distance from N5 FAD to alpha carbon of HMFCA (Å)
HMFH-Thr550Ser3 (Before MD simulation)	1.186	7.940	4.591
HMFH-Thr550Ser3 (After MD simulation)		8.248	6.059
HMFH-Val21Cys3 (Before MD simulation)	1.288	6.258	4.529
HMFH-Val21Cys3 (After MD simulation)		10.873	7.158

HMFH_Asp200Thr-Tyr209Val (Before MD simulation)	1.102	7.179	4.561
HMFH_Asp200Thr-Tyr209Val (After MD simulation)		9.576	4.263
HMFH_Met58Pro3 (Before MD simulation)	1.306	6.431	4.404
HMFH_Met58Pro3 (After MD simulation)		11.160	7.904
HMFH_Ser204GlyTyr209 Val (Before MD simulation)	1.135	5.731	4.846
HMFH_Ser204GlyTyr209 Val (After MD simulation)		11.102	9.028
HMFHfadHMFCA_D46G (Before MD simulation)	1.307	12.814	11.689
HMFHfadHMFCA_D46G (After MD simulation)		12.267	13.391

The above data offer valuable insights into the structural changes induced by protein mutations and their effects on protein-ligand interactions. The Calpha RMSD values represent the root mean square deviation between the structures before and after molecular dynamics (MD) simulations, indicating the extent of structural changes caused by the mutations. Higher RMSD values suggest greater structural deviations, indicating significant alterations in the protein's overall conformation due to the mutations. For instance, the HMFH-Val21Cys and HMFH_Met58Pro mutants exhibit notably higher RMSD values after MD simulations compared to before, indicating substantial structural rearrangements induced by these mutations.

Additionally, the distances measured from key protein-ligand interaction sites provide insights into the impact of mutations on these interactions. For example, the distance from the His N position to the proton from the OH group of HMFCA reflects the proximity between the catalytic residue (Histidine) and the substrate (HMFCA). Changes in this distance may indicate alterations in the enzyme's ability to catalyze the reaction, potentially affecting its efficiency. Similarly, the distance from N5 FAD to the alpha carbon of HMFCA indicates the proximity between the enzyme's cofactor (FAD) and the substrate. Alterations in this distance could influence the enzyme-substrate interaction and the catalytic mechanism (Appendix Table A1).

Overall, these structural changes and alterations in protein-ligand interactions shed light on the functional consequences of mutations on enzyme activity and substrate specificity. Understanding these changes is crucial for elucidating the molecular basis of enzyme function and for guiding rational enzyme engineering efforts aimed at optimizing biocatalytic processes for various industrial applications.

After performing agarose gel electrophoresis of the gradient PCR products, it showed amplification for all mutants except the mutant HMFH V21C (Fig: 10).

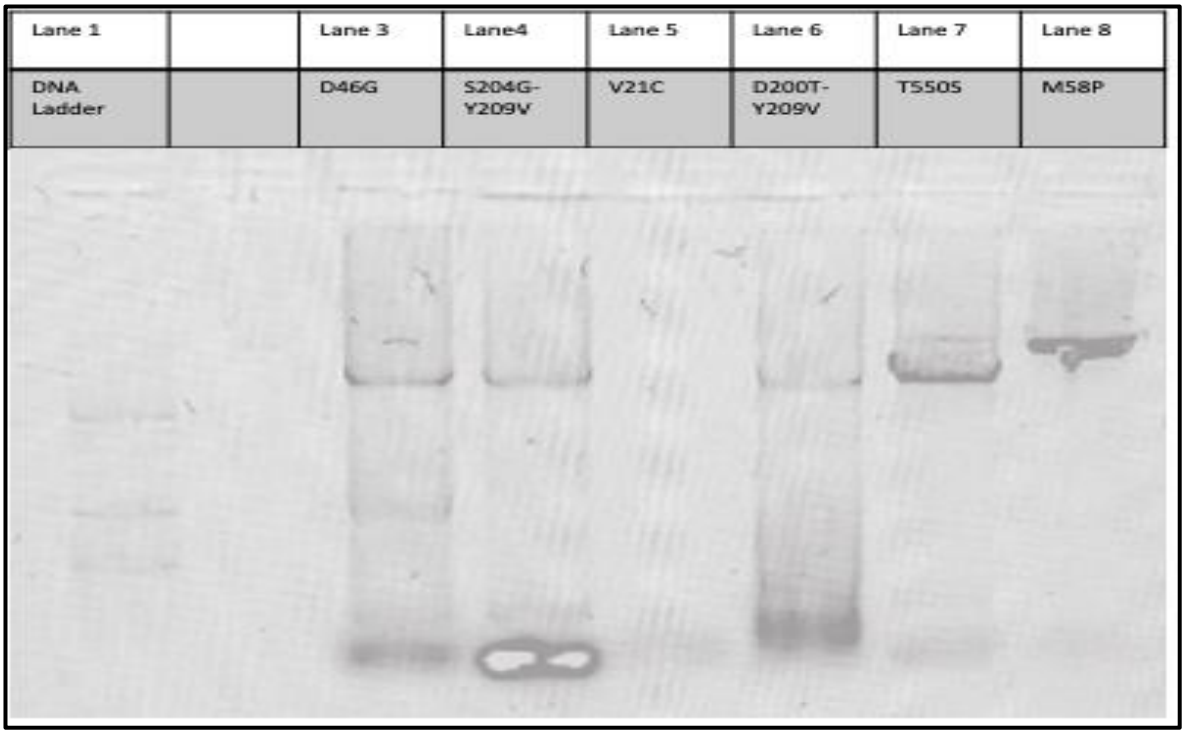

Fig 10: Agarose gel electrophoresis for the HMFH mutants

To confirm the presence of MBP the restriction enzymes Nde1 and Not1 were used, it resulted in the formation of 2 fragments one of HMFH and rest of the plasmid (Fig: 11). The HMFH mutants M1, M2, M4, M5 and M6 were sent for sequencing to Eurofins.

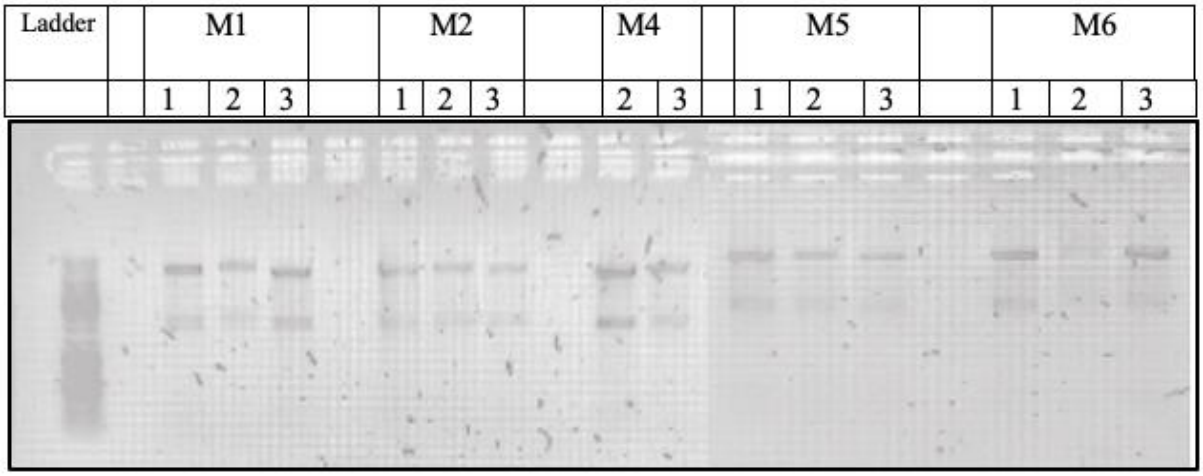

Fig 11: Agarose gel electrophoresis Upper: L1 – Ladder, L3 – Mutant 1-1, L4 – Mutant 1-2, L5 – Mutant 1-3, L7 – Mutant 2-1, L8 – Mutant 2-2, L9 – Mutant 2-3, L11 – Mutant 4-2, L12 – Mutant 4-3. Lower: L2 – Mutant 5-1, L3 – Mutant 5-2, L4 – Mutant 5-3, L6 – Mutant 6-1, L7 – Mutant 6-2, L8 – Mutant 6-3. HMFH 1740 BP Rest fragment 5718 Total 7458bp.

Out of the five mutants tested, the sequence of mutants T550S and M58P matched the sequencing results. Hence, these two mutants were selected for HPLC analysis. A comparative assessment was performed between HMFH mutants and the wild type regarding their efficiency in oxidizing HMFCA, as well as their production of FFCA and FDCA, using HPLC analysis. This was conducted in a deep well 2 mL reaction setup. Samples of 20 µL were withdrawn at intervals of 0, 1, 3, 10, 24, and 48 hours for subsequent analysis using HPLC.

The reaction mixtures included:

i.	HMFCA (2 mg/mL)		+ FAD (50 µM)
ii.	HMFCA (2 mg/mL)		
iii.	HMFH WT	+ HMFCA (2 mg/mL)	+ FAD (50 µM)
iv.	HMFH T550S	+ HMFCA (2 mg/mL)	+ FAD (50 µM)
v.	HMFH M58P	+ HMFCA (2 mg/mL)	+ FAD (50 µM)
vi.	HMFH WT	+ HMFCA (2 mg/mL)	
vii.	HMFH T550S	+ HMFCA (2 mg/mL)	
viii.	HMFH M58P	+ HMFCA (2 mg/mL)	

These setups allowed for the monitoring of enzymatic activity over time and the comparison of conversion rates under various conditions.

Table 5: Change in pH before and after the reaction

Reaction	Before pH	After pH
HMFCA (2mg/mL) + FAD 50 µM	7.70	7.83
HMFCA (2mg/mL)	8	7.67
HMFH WT + HMFCA (2mg/mL) + FAD (50 µM)	7.51	7.78
HMFH T550S + HMFCA (2mg/mL) + FAD (50 µM)	7.50	7.86
HMFH M58P + HMFCA (2mg/mL) + FAD (50 µM)	7.70	8.57
HMFH WT + HMFCA (2mg/mL)	7.62	7.69
HMFH T550S + HMFCA (2mg/mL)	7.33	7.85
HMFH M58P + HMFCA (2mg/mL)	7.42	8.52

The pH of the reaction before and after didn't show much change (Table 5).

7.8 Compare the activity of wild type and mutants with/without FAD:

After 24 hours, there was around 65% oxidation of HMFCA using the HMFH MBP wild type, while the Thr550Ser mutant showed 50% oxidation and the Met58Pro mutant showed around 20% oxidation. After 48 hours, 100% oxidation was observed for the wild type and 86% for Thr550Ser, while no significant change was noticed for Met58Pro. Importantly, no significant difference was observed when the enzyme was used with or without the cofactor FAD, indicating that the presence of FAD did not substantially affect the enzymatic activity

in this context. This could be because the enzyme likely reached its maximum activity without additional FAD, suggesting saturation under the experimental conditions.(Fig: 12).

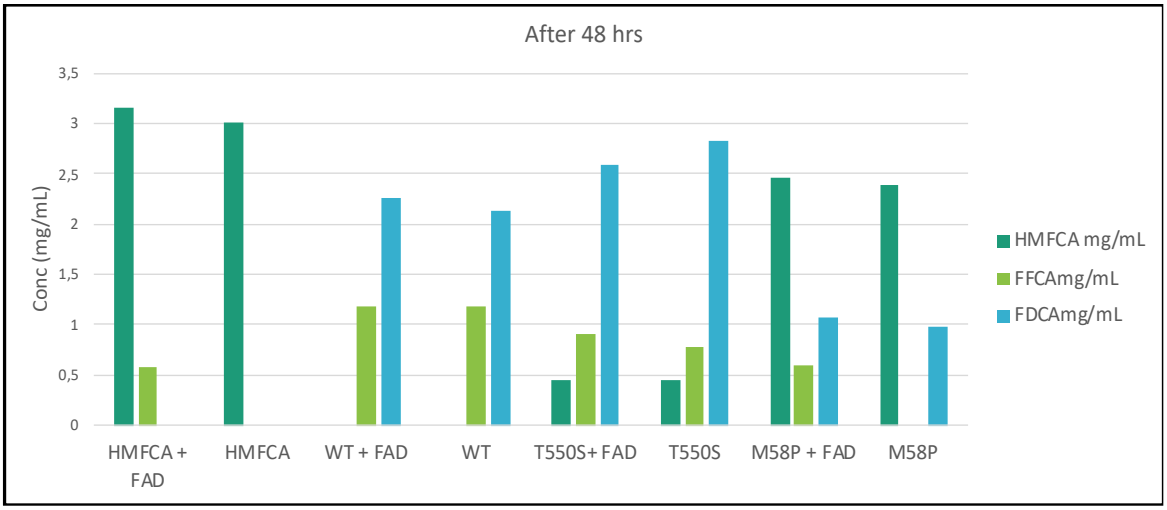

Fig 12: Column chart showing the concentrations of HMFCA, FFCA, FDCA after 48 hours) with HMFH wild type, HMFH mutant T550S (M5), HMFH mutant M58P (M6), and without the HMFH enzyme in the presence of cofactor FAD.

These findings highlight the varying catalytic capabilities of the wild type and mutant enzymes, with the wild type exhibiting the highest activity followed by the Thr550Ser mutant and the Met58Pro mutant displaying the lowest activity. The choice of a serine substitution for threonine at position 550 preserves the hydroxyl group, which is crucial for potential hydrogen bonding interactions and maintains some similarity in size and polarity. This selection likely aimed to subtly alter the active site geometry and hydrogen bonding network, providing insights into the specific role of Thr550 in substrate binding and catalysis. Conversely, the replacement of methionine at position 58 with proline introduces a stark contrast in the amino acid properties, transitioning from a flexible, sulfur-containing residue to a rigid, cyclic amino acid. The proline substitution disrupts the local protein backbone, potentially causing significant structural alterations within the active site region. This deliberate choice aimed to assess the importance of Met58 in maintaining overall structural integrity and flexibility crucial for proper substrate orientation and catalysis These structural changes underscore the importance of Thr550 and Met58 residues in maintaining the enzyme's catalytic function and provide valuable insights into the structural and mechanistic determinants of catalysis and how even small changes can have big effects on HMFH MBP activity.

The comparison between the reactions with and without FAD revealed no substantial difference in behavior. However, contrasting the wild type with the Thr550Ser and Met58Pro mutants, significant variations were noted (Fig:13).

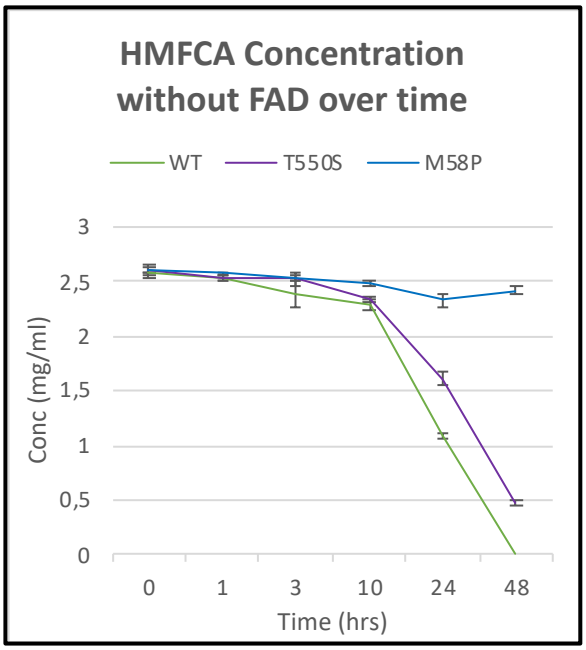

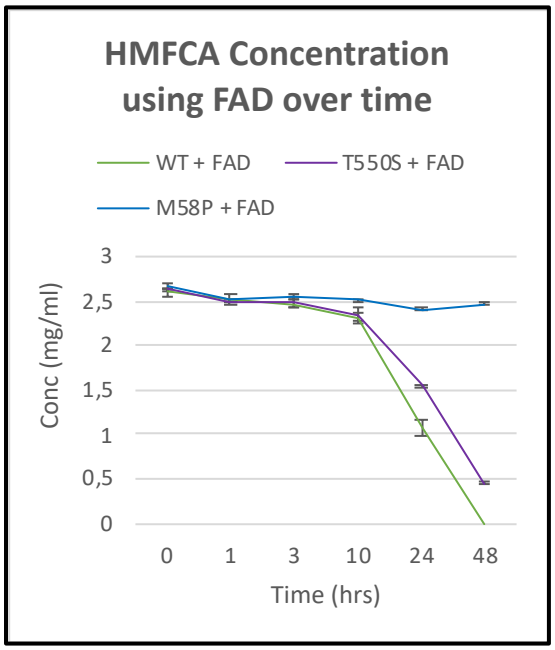

Fig 13: Error plot depicting the concentrations of HMFCA at various time points (0, 1, 3, 10, 24, and 48 hours) in the presence of HMFH Wild type, HMFH mutant Thr550Ser, HMFH mutant Met58Pro, without FAD (left) and with FAD (right).

The data indicates that the wild-type enzyme, HMFH, exhibited minimal change in substrate oxidation regardless of the presence of the cofactor FAD. Moreover, there was a significant reduction in HMFCA concentration after 10 hours, with complete depletion observed after 48 hours using the wild-type enzyme (Fig: 14).

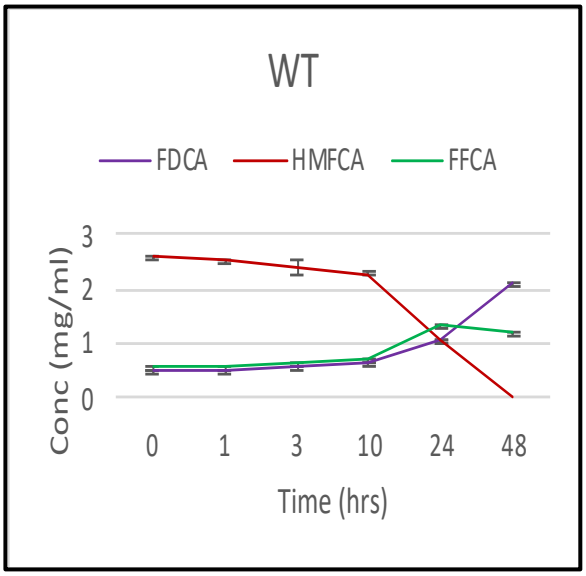

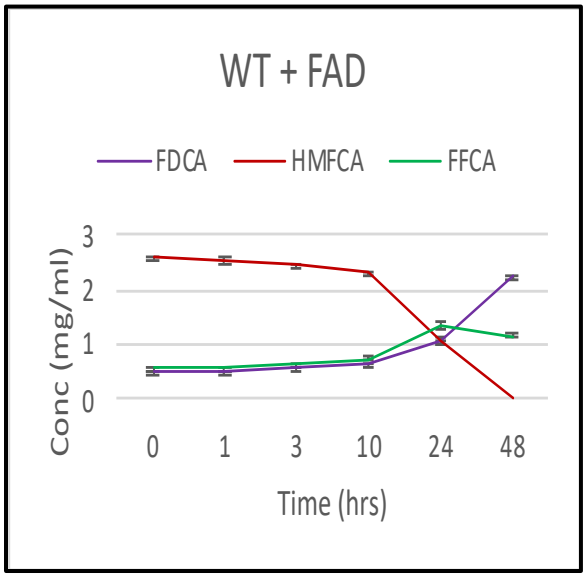

Fig 14: Error plot representing the variations in HMFCA oxidation and the generation of FFCA and FDCA at different time points (0, 1, 3, 10, 24, and 48 hours) using the HMFH Wild Type (WT) without FAD (left) and with FAD (right).

It was observed that there was minimal change in the oxidation of the substrate HMFCA, regardless of the presence or absence of the cofactor FAD. Additionally, the concentration of HMFCA showed a significant reduction even after 48 hours using HMFH mutant Thr550Ser. However, it was not completely oxidized compared to the wild type. This could be attributed to potential structural or functional differences in the mutant enzyme, affecting its efficiency in substrate binding and catalysis. It was observed that this mutant performs differently in terms of substrate utilization the HMFCA and product formation, it suggests that the mutation has a significant impact on enzyme function (Fig: 15).

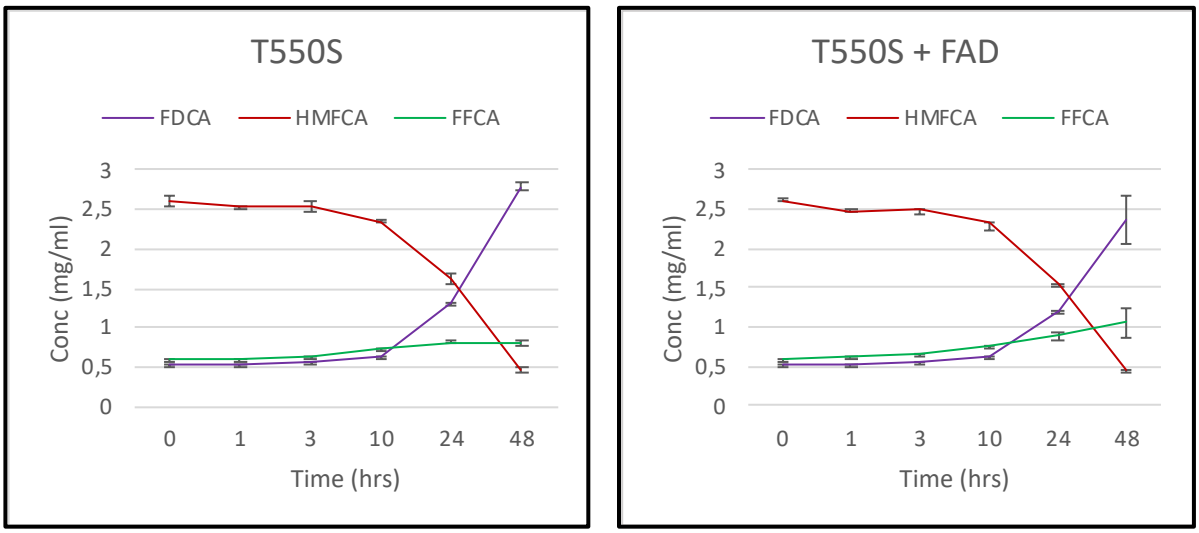

Fig 15: Error plot representing the variations in HMFCA oxidation and the generation of FFCA and FDCA at different time points (0, 1, 3, 10, 24, and 48 hours) using the HMFH mutant Thr550Ser without FAD (left) and with FAD (right).

It was noted that there was negligible alteration in the oxidation of the substrate HMFCA with or without the use of the cofactor FAD. Furthermore, the concentration of HMFCA exhibited minimal reduction even after 48 hours. This could be attributed to the HMFH mutant Met58Pro enzyme's inability to fully bind to the substrate (Fig 16).

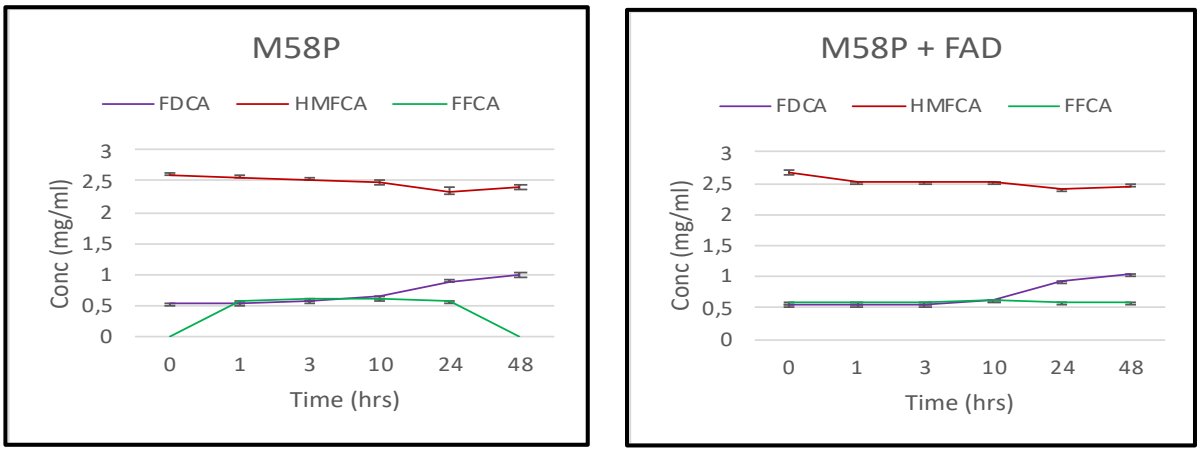

Fig 16: Error plot representing the variations in HMFCA oxidation and the generation of FFCA and FDCA at different time points (0, 1, 3, 10, 24, and 48 hours) using the HMFH mutant Met58Pro without FAD (left) and with FAD (right).

7.9 Mutant Colony Screening and Sequencing Analysis:

Around 5 colonies from each mutants D46G, Ser204Gly-Tyr209Val, Asp200Thr-Tyr209Val were picked up and spotted on LB agar plate containing Ampicillin 100 mg/mL. After sequencing, it was found that the sequencing completely matched with D46G mutation. However, only half of the Tyr209Val mutation was found to match with the Asp200Thr-Tyr209Val mutation.

8 Discussion:

The consistent behavior observed between reactions with and without FAD suggests that the enzyme likely reached maximal activity without the need for additional FAD, indicating saturation under the experimental conditions. This implies that the enzyme's activity is not significantly influenced by the presence or absence of the cofactor within the tested parameters.

Compared to the wild type, the Thr550Ser mutation doesn't exhibit the same level of efficiency. However, it does demonstrate some ability for substrate binding, as evidenced by its near-complete oxidation of HMFCA. This suggests that the mutation induces structural changes that alter the enzyme's active site for moderate substrate interaction. Combining the Thr550Ser mutation with other beneficial mutations could potentially further enhance the enzyme's catalytic activity.

Conversely, the Met58Pro mutation has a negative impact on substrate conversion, resulting in minimal HMFCA oxidation. This indicates that the Met58Pro mutation disrupts the enzyme's structure in a way that impairs its catalytic function. Exploring alternative mutations at this position, such as Met58Ala, Met58Val, or Met58Leu, could potentially maintain structural integrity while enhancing catalytic activity.

The wild-type (WT) enzyme may inherently possess kinetic properties, such as Km and kcat, that are better suited for HMFCA conversion compared to the mutated versions. These properties enable the WT enzyme to achieve efficient catalysis under the given conditions. Mutations, while aimed at improving function, might inadvertently alter these kinetic properties, leading to less efficient catalysis overall.

In summary, the findings highlight the delicate balance between structural modifications and enzyme activity. While certain mutations, like Thr500Ser, may not enhance enzyme function, they may still exhibit some activity. Conversely, others, like Met58Pro, may have detrimental effects. These insights are crucial for guiding future efforts in enzyme engineering, aiming to achieve optimal catalytic properties for biotechnological and industrial applications.

9 Conclusion:

The study identified that a concentration of 2 mg/mL of HMFCA was optimal for achieving the highest HMFH (HMF/furfural oxidoreductase) activity. This concentration allowed the enzyme to perform at its best under the experimental conditions provided, ensuring maximal catalytic efficiency.

When comparing different growth medium, TB (Terrific Broth) medium supported better enzyme activity than LB (Luria-Bertani) medium. This suggests that the nutrients and

conditions in TB medium are more conducive to enzyme stability and function, leading to higher overall activity levels.

The HMFH MBP (maltose-binding protein) fusion exhibited the highest catalytic efficiency when compared to other tagged variants of the enzyme. This indicates that the MBP tag may play a role in solubilizing the enzyme or facilitating better substrate interactions, making it the most effective construct among those tested.

In terms of conversion rates, whole cell systems provided the best performance. Using whole cells likely offers a more natural environment for the enzyme, possibly due to factors such as cellular cofactors, proper folding, and optimal microenvironments that are not replicated in purified enzyme systems.

The Thr550Ser mutation exhibited a moderate ability to bind to the substrate, though not as much as the wild type. Nevertheless, it nearly completely converted HMFCA, suggesting it alters how the enzyme interacts with and transforms the substrate. Compared to the wild type, this mutation may not be as effective in modifying the enzyme's structure to facilitate more efficient binding and catalysis. On the other hand, the Met58Pro mutation showed a considerable reduction in substrate conversion. This finding indicates that Met58 is a critical residue for maintaining proper substrate affinity. The Met58Pro mutation likely disrupts the enzyme’s active site geometry or affects critical catalytic residues, impairing its ability to effectively bind and convert HMFCA.

Overall, these findings highlight the importance of optimizing various factors, including enzyme concentration, growth medium, enzyme constructs, and specific mutations, to enhance enzyme performance.

10 Future work:

To continue enhancing the catalytic efficiency and substrate affinity of the enzyme, additional mutation testing could focus on the D46G, S204G-Y209V, Y209V and V21C mutations. These mutations have been identified based on previous studies and computational predictions as potentially beneficial for improving enzyme function. Testing these mutations individually and in combination will provide insights into their effects on enzyme stability, activity, and overall performance. This step is crucial for determining how these specific amino acid changes influence the enzyme's structural and catalytic properties, guiding further engineering efforts.

A targeted approach will involve combinatorial mutagenesis, specifically integrating the Thr550Ser mutation with nearby residue mutations. The goal is to maximize enzyme activity and specificity by exploring synergistic effects between multiple mutations. The Thr550Ser mutation has already shown promise by exhibiting some substrate-binding affinity. By combining it with other strategically selected mutations, there is potential to further enhance the enzyme's catalytic efficiency. This combinatorial strategy aims to identify optimal mutation sets that work together to enhance the enzyme's performance beyond what can be achieved by individual mutations alone.

The Met58 residue has proven to be critical for substrate conversion, as evidenced by the significant reduction in activity observed with the Met58Pro mutation. Therefore, further investigation into Met58 mutations is essential to identify optimal substitutions that maintain

or enhance structural integrity while improving catalytic activity. Potential substitutions like Met58Ala, Met58Val, or Met58Leu could be explored to determine their effects on the enzyme's active site geometry and overall function. This research will help identify mutations that retain the beneficial aspects of Met58 while mitigating any negative impacts on enzyme activity.

To efficiently identify the best combinations of mutations for enhanced enzyme activity, high-throughput screening methods will be implemented. These techniques allow for the rapid assessment of a large number of mutant variants, providing a comprehensive understanding of how different mutations interact and contribute to enzyme performance. High-throughput screening will facilitate the discovery of optimal mutation combinations that yield the highest catalytic efficiency and substrate specificity, significantly accelerating the enzyme engineering process. By integrating these advanced screening methods, it can systematically evaluate and refine enzyme variants to achieve desired improvements in biocatalytic applications.

11 References:

1. Chairat S, Gheewala SH. Life cycle assessment and circularity of polyethylene terephthalate bottles via closed and open loop recycling. Environ Res. 2023;236(Pt 1):116788.
2. de Jong E, Visser HRA, Dias AS, Harvey C, Gruter GM. The Road to Bring FDCA and PEF to the Market. Polymers (Basel). 2022;14(5).
3. Fei X, Wang J, Zhang X, Jia Z, Jiang Y, Liu X. Recent Progress on Bio-Based Polyesters Derived from 2,5-Furandicarbonxylic Acid (FDCA). Polymers (Basel). 2022;14(3).
4. Chandra S, Walsh KB. Microplastics in water: Occurrence, fate and removal. J Contam Hydrol. 2024;264:104360.
5. Cowger W, Willis KA, Bullock S, Conlon K, Emmanuel J, Erdle LM, et al. Global producer responsibility for plastic pollution. Sci Adv. 2024;10(17):eadj8275.
6. de Deus BCT, Costa TC, Altomari LN, Brovini EM, de Brito PSD, Cardoso SJ. Coastal plastic pollution: A global perspective. Mar Pollut Bull. 2024;203:116478.
7. Patel SKS, Lee JK. Plastic Eating Enzymes: A Step Towards Sustainability. Indian J Microbiol. 2022;62(4):658-61.
8. Safdar A, Ismail F, Safdar M, Imran M. Eco-friendly approaches for mitigating plastic pollution: advancements and implications for a greener future. Biodegradation. 2024.
9. Wei XF, Yang W, Hedenqvist MS. Plastic pollution amplified by a warming climate. Nat Commun. 2024;15(1):2052.
10. Zaini N, Kasmuri N, Mojiri A, Kindaichi T, Nayono SE. Plastic pollution and degradation pathways: A review on the treatment technologies. Heliyon. 2024;10(7):e28849.
11. Bagnani M, Peydayesh M, Knapp T, Appenzeller E, Sutter D, Kranzlin S, et al. From Soy Waste to Bioplastics: Industrial Proof of Concept. Biomacromolecules. 2024;25(3):2033-40.
12. Barcelo D. Microplastics in the environment: analytical chemistry methods, sorption materials, risks and sustainable solutions. Anal Bioanal Chem. 2024.
13. Elkaliny NE, Alzamel NM, Moussa SH, Elodamy NI, Madkor EA, Ibrahim EM, et al. Macroalgae Bioplastics: A Sustainable Shift to Mitigate the Ecological Impact of Petroleum-Based Plastics. Polymers (Basel). 2024;16(9).
14. Lima GMR, Mukherjee A, Picchioni F, Bose RK. Characterization of Biodegradable Polymers for Porous Structure: Further Steps toward Sustainable Plastics. Polymers (Basel). 2024;16(8).

15. Sanchez-Ruiz MI, Martinez AT, Serrano A. Optimizing operational parameters for the enzymatic production of furandicarboxylic acid building block. Microb Cell Fact. 2021;20(1):180.
16. Ali SS, Abdelkarim EA, Elsamahy T, Al-Tohamy R, Li F, Kornaros M, et al. Bioplastic production in terms of life cycle assessment: A state-of-the-art review. Environ Sci Ecotechnol. 2023;15:100254.
17. Atiwesh G, Mikhael A, Parrish CC, Banoub J, Le TT. Environmental impact of bioplastic use: A review. Heliyon. 2021;7(9):e07918.
18. Karan H, Funk C, Grabert M, Oey M, Hankamer B. Green Bioplastics as Part of a Circular Bioeconomy. Trends Plant Sci. 2019;24(3):237-49.
19. Kong U, Mohammad Rawi NF, Tay GS. The Potential Applications of Reinforced Bioplastics in Various Industries: A Review. Polymers (Basel). 2023;15(10).
20. Serrano-Aguirre L, Prieto MA. Can bioplastics always offer a truly sustainable alternative to fossil-based plastics? Microb Biotechnol. 2024;17(4):e14458.
21. Varghese S, Dhanraj ND, Rebello S, Sindhu R, Binod P, Pandey A, et al. Leads and hurdles to sustainable microbial bioplastic production. Chemosphere. 2022;305:135390.
22. Viera JSC, Marques MRC, Nazareth MC, Jimenez PC, Sanz-Lazaro C, Castro IB. Are biodegradable plastics an environmental rip off? J Hazard Mater. 2021;416:125957.
23. Pham NN, Chen CY, Li H, Nguyen MTT, Nguyen PKP, Tsai SL, et al. Engineering Stable Pseudomonas putida S12 by CRISPR for 2,5-Furandicarboxylic Acid (FDCA) Production. ACS Synth Biol. 2020;9(5):1138-49.
24. Endres HJ. Bioplastics. Adv Biochem Eng Biotechnol. 2019;166:427-68.
25. Vinambres M, Espada M, Martinez AT, Serrano A. Screening and Evaluation of New Hydroxymethylfurfural Oxidases for Furandicarboxylic Acid Production. Appl Environ Microbiol. 2020;86(16).
26. Ardemani L, Cibin G, Dent AJ, Isaacs MA, Kyriakou G, Lee AF, et al. Solid base catalysed 5-HMF oxidation to 2,5-FDCA over Au/hydrotalcites: fact or fiction? Chem Sci. 2015;6(8):4940-5.
27. Cajnko MM, Novak U, Grilc M, Likozar B. Enzymatic conversion reactions of 5-hydroxymethylfurfural (HMF) to bio-based 2,5-diformylfuran (DFF) and 2,5-furandicarboxylic acid (FDCA) with air: mechanisms, pathways and synthesis selectivity. Biotechnol Biofuels. 2020;13:66.
28. Dijkman WP, Fraaije MW. Discovery and characterization of a 5-hydroxymethylfurfural oxidase from Methylovorus sp. strain MP688. Appl Environ Microbiol. 2014;80(3):1082-90.
29. Martin C, Ovalle Maqueo A, Wijma HJ, Fraaije MW. Creating a more robust 5-hydroxymethylfurfural oxidase by combining computational predictions with a novel effective library design. Biotechnol Biofuels. 2018;11:56.
30. Payne KAP, Marshall SA, Fisher K, Cliff MJ, Cannas DM, Yan C, et al. Enzymatic Carboxylation of 2-Furoic Acid Yields 2,5-Furandicarboxylic Acid (FDCA). ACS Catal. 2019;9(4):2854-65.
31. Wu S, Liu Q, Tan H, Zhang F, Yin H. A Novel 2,5-Furandicarboxylic Acid Biosynthesis Route from Biomass-Derived 5-Hydroxymethylfurfural Based on the Consecutive Enzyme Reactions. Appl Biochem Biotechnol. 2020;191(4):1470-82.
32. Ahangar FA, Rashid U, Ahmad J, Tsubota T, Alsalme A. Conversion of Waste Polyethylene Terephthalate (PET) Polymer into Activated Carbon and Its Feasibility to Produce Green Fuel. Polymers (Basel). 2021;13(22).
33. Radley E, Davidson J, Foster J, Obexer R, Bell EL, Green AP. Engineering Enzymes for Environmental Sustainability. Angew Chem Weinheim Bergstr Ger. 2023;135(52):e202309305.

34. Deshan ADK, Atanda L, Moghaddam L, Rackemann DW, Beltramini J, Doherty WOS. Heterogeneous Catalytic Conversion of Sugars Into 2,5-Furandicarboxylic Acid. Front Chem. 2020;8:659.
35. Hsu CT, Kuo YC, Liu YC, Tsai SL. Green conversion of 5-hydroxymethylfurfural to furan-2,5-dicarboxylic acid by heterogeneous expression of 5-hydroxymethylfurfural oxidase in Pseudomonas putida S12. Microb Biotechnol. 2020;13(4):1094-102.
36. Yuan H, Li J, Shin HD, Du G, Chen J, Shi Z, et al. Improved production of 2,5-furandicarboxylic acid by overexpression of 5-hydroxymethylfurfural oxidase and 5-hydroxymethylfurfural/furfural oxidoreductase in Raoultella ornithinolytica BF60. Bioresour Technol. 2018;247:1184-8.
37. Godoy CA, Valderrama P, Furtado AC, Boroski M. Analysis of HMF and furfural in hydrolyzed lignocellulosic biomass by HPLC-DAD-based method using FDCA as internal standard. MethodsX. 2022;9:101774.
38. Yuan H, Liu Y, Li J, Shin HD, Du G, Shi Z, et al. Combinatorial synthetic pathway fine-tuning and comparative transcriptomics for metabolic engineering of Raoultella ornithinolytica BF60 to efficiently synthesize 2,5-furandicarboxylic acid. Biotechnol Bioeng. 2018;115(9):2148-55.
39. Karich A, Kleeberg SB, Ullrich R, Hofrichter M. Enzymatic Preparation of 2,5-Furandicarboxylic Acid (FDCA)-A Substitute of Terephthalic Acid-By the Joined Action of Three Fungal Enzymes. Microorganisms. 2018;6(1).
40. Vina-Gonzalez J, Martinez AT, Guallar V, Alcalde M. Sequential oxidation of 5-hydroxymethylfurfural to furan-2,5-dicarboxylic acid by an evolved aryl-alcohol oxidase. Biochim Biophys Acta Proteins Proteom. 2020;1868(1):140293.
41. Gandomkar S, Jost E, Loidolt D, Swoboda A, Pickl M, Elaily W, et al. Biocatalytic Enantioselective Oxidation of Sec-Allylic Alcohols with Flavin-Dependent Oxidases. Adv Synth Catal. 2019;361(22):5264-71.
42. Han Y, Qu W, Feng W. Coupling a recombinant oxidase to catalase through specific noncovalent interaction to improve the oxidation of 5-hydroxymethylfurfural to 2,5-furandicarboxylic acid. Enzyme Microb Technol. 2021;150:109895.

12 Appendix:

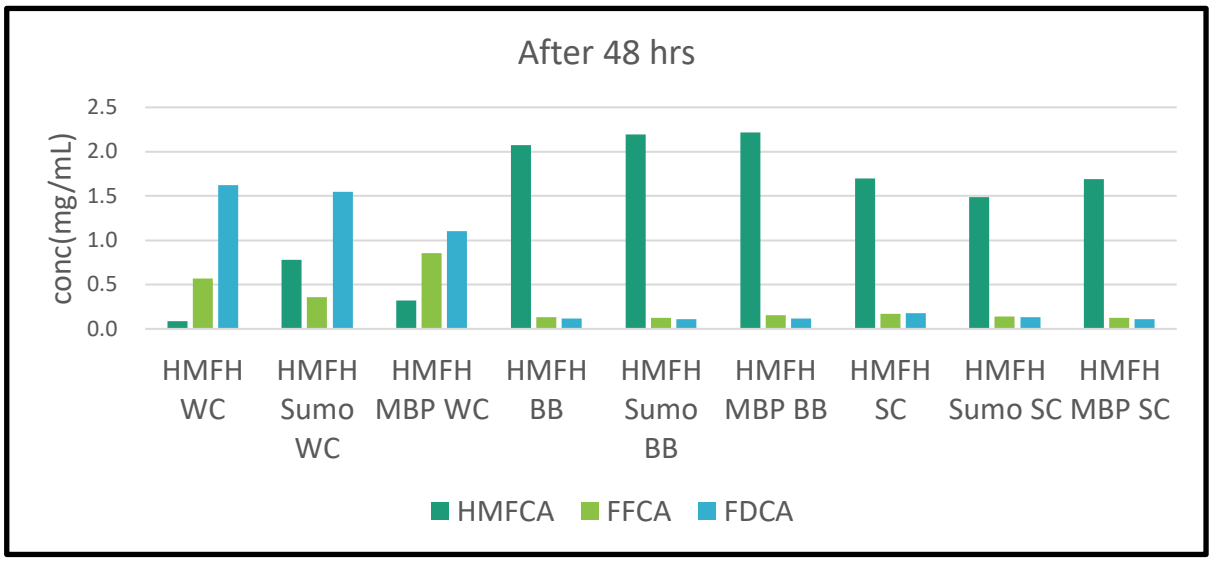

Fig A1: Comparison of HMFCA conversion rates using various lysis methods after 48 hours of incubation in TB medium at 30°C and 200 RPM. (WC: whole cells, BB: BugBuster, SC: Sonicated cells)

Table A1: Structural Changes in Protein Mutations Before and After MD Simulations

Mutation	Binding Pocket
HMFH-Thr550Ser3 (Before MD simulation)	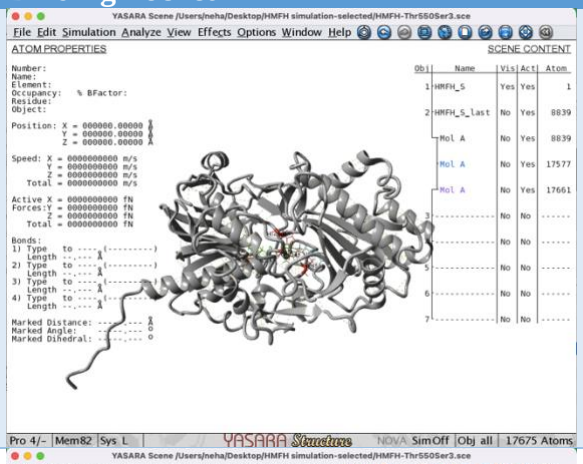
HMFH-Thr550Ser3 (After MD simulation)	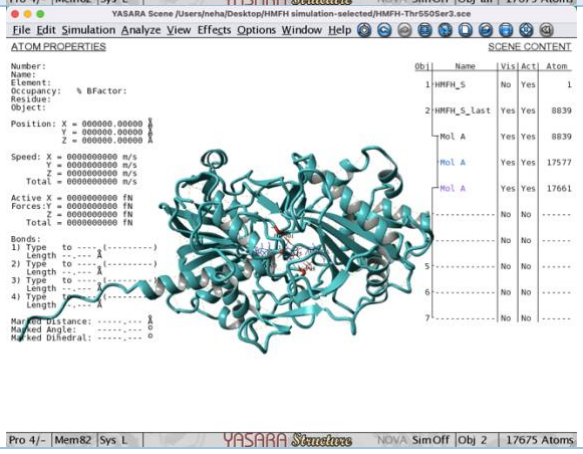

HMFH-Val21Cys3 (Before MD simulation)	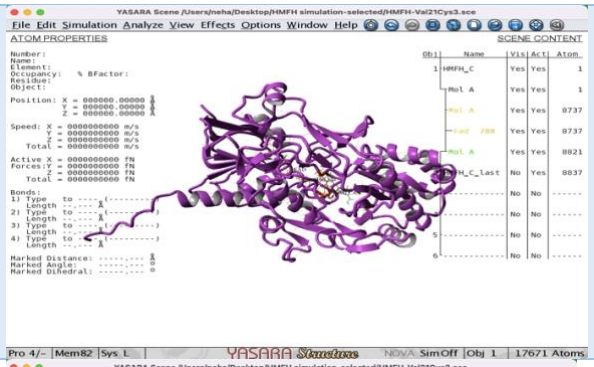
HMFH-Val21Cys3 (After MD simulation)	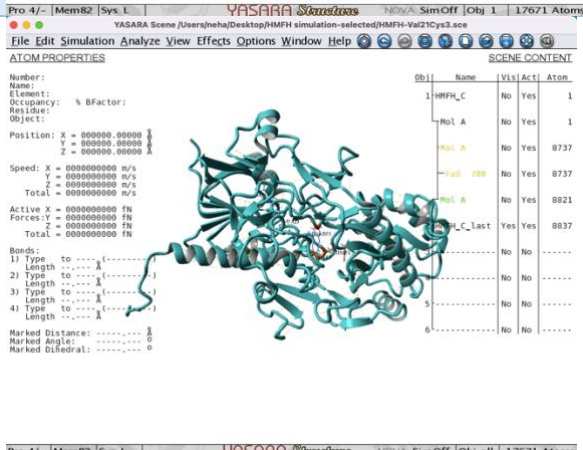
HMFH_Asp200Thr-Tyr209Val3 2 (Before MD simulation)	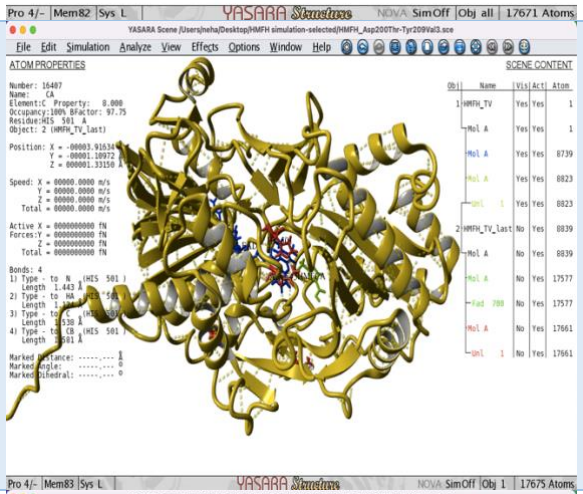
HMFH_Asp200Thr-Tyr209Val3 2 (After MD simulation)	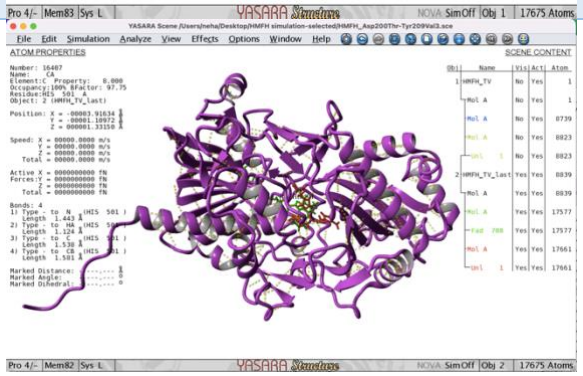

HMFH_Met58Pro3 (Before MD simulation)	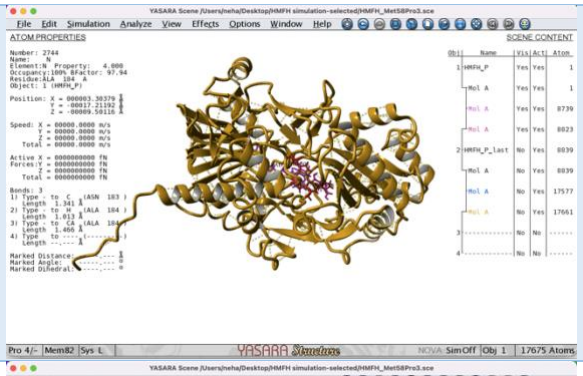
HMFH_Met58Pro3 (After MD simulation)	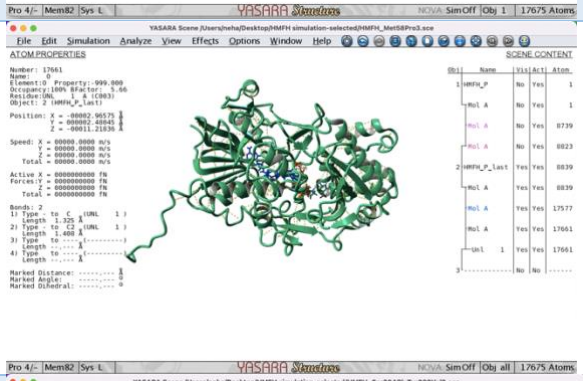
HMFH_Ser204GlyTyr209Val2 (Before MD simulation)	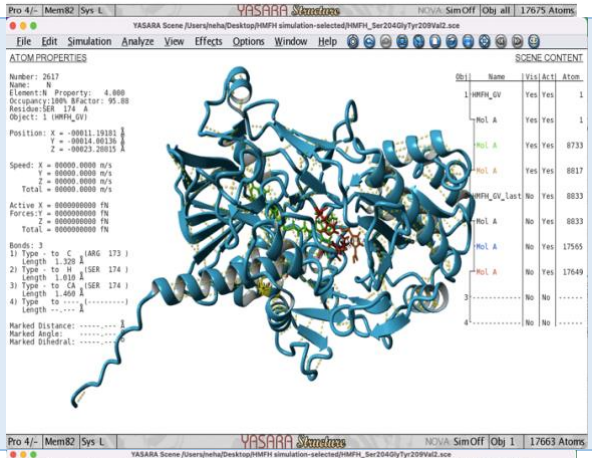
HMFH_Ser204GlyTyr209Val2 (After MD simulation)	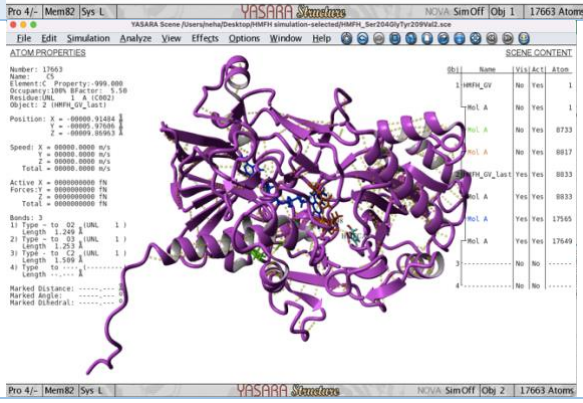

HMFHfadHMFCA_D46G (Before MD simulation)	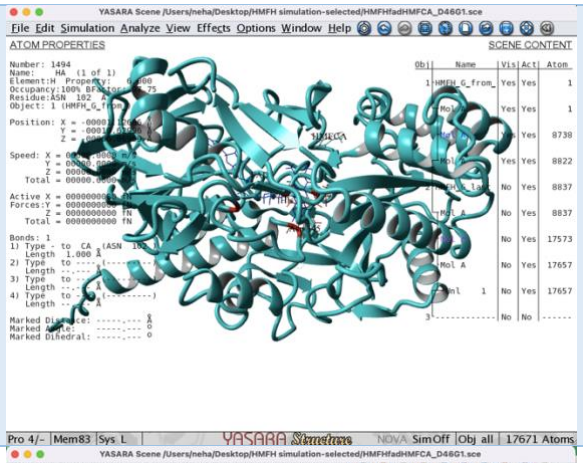
HMFHfadHMFCA_D46G (After MD simulation)	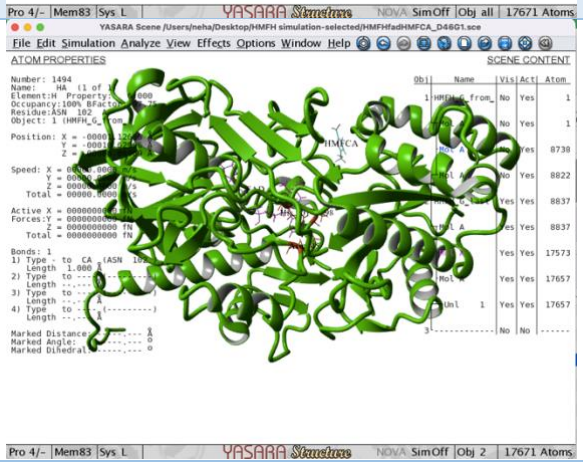

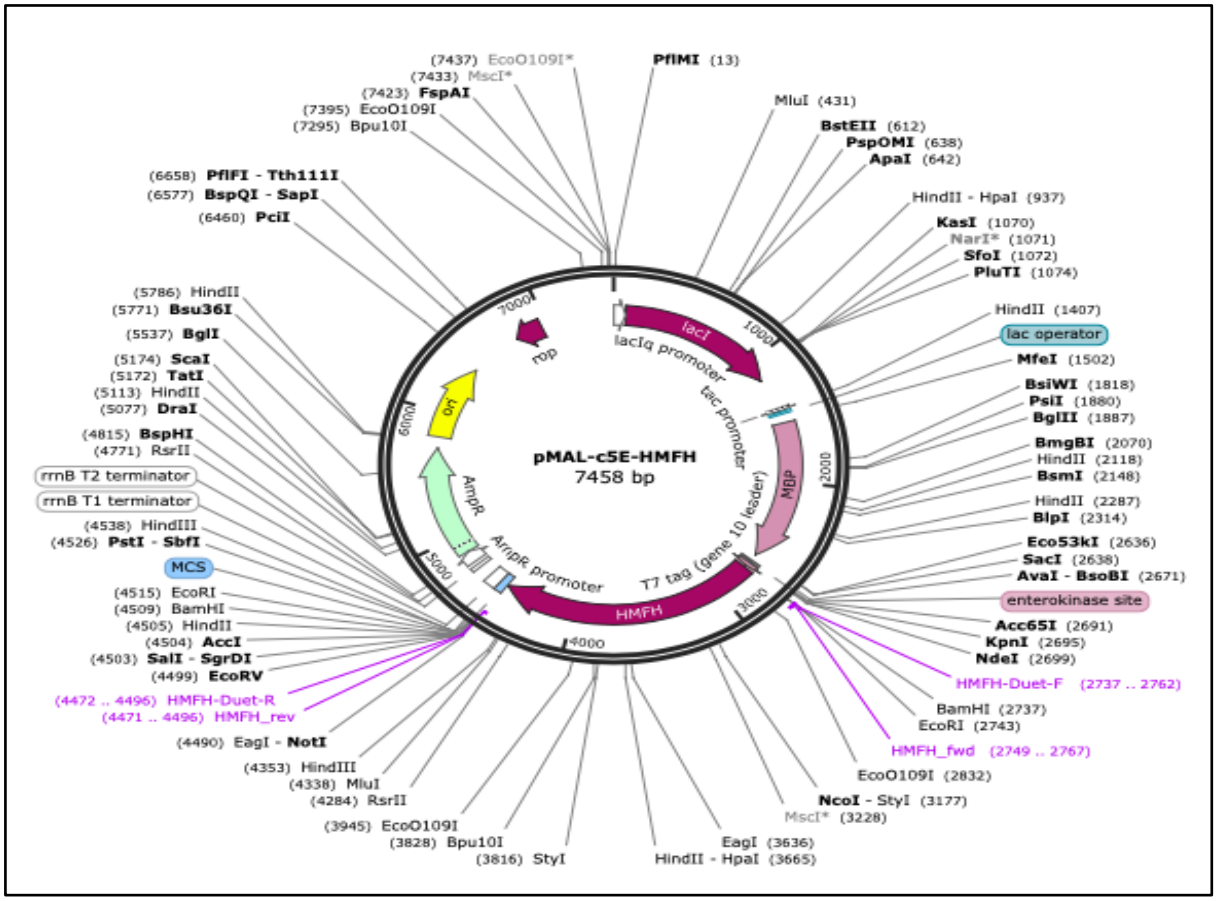

Fig A2: Circular map of HMFH MBP using SnapGene Viewer